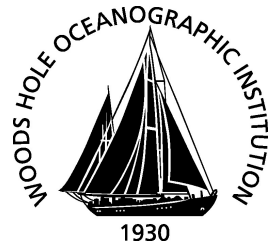


Massachusetts Institute of Technology
Woods Hole Oceanographic Institution



**Joint Program
in Oceanography/
Applied Ocean Science
and Engineering**



DOCTORAL DISSERTATION

Form, function and flow in the plankton:
Jet propulsion and filtration by pelagic tunicates

by

Kelly Rakow Sutherland

February 2010

Report Documentation Page				Form Approved OMB No. 0704-0188	
Public reporting burden for the collection of information is estimated to average 1 hour per response, including the time for reviewing instructions, searching existing data sources, gathering and maintaining the data needed, and completing and reviewing the collection of information. Send comments regarding this burden estimate or any other aspect of this collection of information, including suggestions for reducing this burden, to Washington Headquarters Services, Directorate for Information Operations and Reports, 1215 Jefferson Davis Highway, Suite 1204, Arlington VA 22202-4302. Respondents should be aware that notwithstanding any other provision of law, no person shall be subject to a penalty for failing to comply with a collection of information if it does not display a currently valid OMB control number.					
1. REPORT DATE FEB 2010		2. REPORT TYPE		3. DATES COVERED	
4. TITLE AND SUBTITLE Form, function and flow in the plankton: Jet propulsion and filtration by pelagic tunicat				5a. CONTRACT NUMBER	
				5b. GRANT NUMBER	
				5c. PROGRAM ELEMENT NUMBER	
6. AUTHOR(S)				5d. PROJECT NUMBER	
				5e. TASK NUMBER	
				5f. WORK UNIT NUMBER	
7. PERFORMING ORGANIZATION NAME(S) AND ADDRESS(ES) Woods Hole Oceanographic, Woods Hole, MA, 02543				8. PERFORMING ORGANIZATION REPORT NUMBER	
9. SPONSORING/MONITORING AGENCY NAME(S) AND ADDRESS(ES)				10. SPONSOR/MONITOR'S ACRONYM(S)	
				11. SPONSOR/MONITOR'S REPORT NUMBER(S)	
12. DISTRIBUTION/AVAILABILITY STATEMENT Approved for public release; distribution unlimited.					
13. SUPPLEMENTARY NOTES					
14. ABSTRACT					
15. SUBJECT TERMS					
16. SECURITY CLASSIFICATION OF:			17. LIMITATION OF ABSTRACT	18. NUMBER OF PAGES 102	19a. NAME OF RESPONSIBLE PERSON
a. REPORT unclassified	b. ABSTRACT unclassified	c. THIS PAGE unclassified			

MIT/WHOI

2010-01

**Form, function and flow in the plankton:
Jet propulsion and filtration by pelagic tunicates**

by

Kelly Rakow Sutherland

Massachusetts Institute of Technology
Cambridge, Massachusetts 02139

and

Woods Hole Oceanographic Institution
Woods Hole, Massachusetts 02543

February 2010

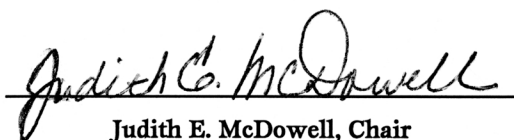
DOCTORAL DISSERTATION

Funding was provided by the National Science Foundation, Massachusetts Institute of Technology, WHOI Ocean Life Institute, an Ocean Ventures Fund award, and the Woods Hole Oceanographic Institution Academic Programs Office.

Reproduction in whole or in part is permitted for any purpose of the United States Government. This thesis should be cited as: Kelly Rakow Sutherland, 2009. Form, function and flow in the plankton: Jet propulsion and filtration by pelagic tunicates. Ph.D. Thesis. MIT/WHOI, 2010-01.

Approved for publication; distribution unlimited.

Approved for Distribution:

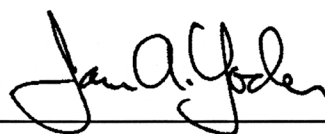


Judith E. McDowell, Chair

Department of Biology



Ed Boyle
MIT Director of Joint Program



James A. Yoder
WHOI Dean of Graduate Studies

**Form, function and flow in the plankton:
Jet propulsion and filtration by pelagic tunicates**

by
Kelly Rakow Sutherland

B.S., Tufts University, 1999
M.S., University of South Alabama, 2004

Submitted in partial fulfillment of the requirements for the degree of
Doctor of Philosophy
at the
MASSACHUSETTS INSTITUTE OF TECHNOLOGY
and the
WOODS HOLE OCEANOGRAPHIC INSTITUTION

February 2010

© 2010 Kelly Rakow Sutherland. All rights reserved.

The author hereby grants to MIT and WHOI permission to reproduce and
to distribute publicly paper and electronic copies of this thesis document
in whole or in part in any medium now known or hereafter created.

Author

Kelly Rakow Sutherland

Joint Program in Oceanography/Applied Ocean Science and Engineering
Massachusetts Institute of Technology
and Woods Hole Oceanographic Institution
October 23, 2009

Certified by

Laurence P. Madin

Laurence P. Madin
Thesis Supervisor

Accepted by

[Signature]

Simon R. Thorrold
Chair, Joint Committee for Biological Oceanography
Woods Hole Oceanographic Institution

Form, function and flow in the plankton: Jet propulsion and filtration by pelagic tunicates

by
Kelly Rakow Sutherland

Submitted to the Department of Biology
on October 23, 2009 in partial fulfillment of the
requirements for the Degree of Doctor of Philosophy in
Biological Oceanography

Abstract

Trade-offs between filtration rate and swimming performance among several salp species with distinct morphologies and swimming styles were compared. Small-scale particle encounter at the salp filtering apparatus was also explored. Observations and experiments were conducted at the Liquid Jungle Lab, off the pacific coast of Panama in January 2006 through 2009. First, time-varying body volume was calculated by digitizing salp outlines from *in situ* video sequences. The resulting volume flow rates were higher than previous measurements, setting an upper limit on filtration capacity. Though each species possessed a unique combination of body kinematics, normalized filtration rates were comparable across species, with the exception of significantly higher rates in *Weelia cylindrica* aggregates, suggesting a tendency towards a flow optimum. Secondly, a combination of *in situ* dye visualization and particle image velocimetry (PIV) measurements were used to describe properties of the jet wake and swimming performance variables including thrust, drag and propulsive efficiency. All species investigated swam via vortex ring propulsion. Though *Weelia cylindrica* was the fastest swimmer, *Pegea confoederata* was the most efficient, producing the highest weight-specific thrust and whole-cycle propulsive efficiency. Weak swimming performance parameters in *Cyclosalpa affinis*, including low weight-specific thrust and low propulsive efficiency, may be compensated by comparatively low energetic requirements. Finally, a low Reynolds number mathematical model using accurately measured parameters and realistic oceanic particle size concentrations showed that submicron particles are encountered at higher rates than larger particles. Results from feeding experiments with 0.5, 1 and 3 μm polystyrene microspheres corroborated model predictions. Though 1 to 10 μm -sized particles (e.g. flagellates, small diatoms) are predicted to provide four times as much carbon as 0.1 to 1 μm - sized particles (e.g. bacteria, *Prochlorococcus*), particles smaller than the mesh size (1.4 μm) can still fully satisfy salp energetic needs.

Thesis Supervisor: Laurence P. Madin

Title: Senior Scientist and Director of Research, WHOI

Acknowledgements

First and foremost, I want to thank my thesis advisor, Larry Madin, for guiding me along the road of salp research. His years of experience doing field research with oceanic plankton give him a broad perspective that I hope to emulate as my career progresses. I really appreciate and admire his sense of adventure as well as his ability to stay composed in pretty much any scenario. I had a supportive and knowledgeable committee who also happen to be Woods Hole alums (Joint Program and BUMP). Alex Techet spent time showing me how to process PIV data and was also bold enough to join me on one of my research trips to Panama. I really enjoyed working with an engineer in the field, especially one who can SCUBA dive and is as easygoing as Alex. Erik Anderson is a physics teacher to the core and has a way of bringing things back to basic principles. As a biologist trying to do fluid mechanics, I really appreciated his patience in leading me through some of the essential concepts. Tony Moss was there for my first trip to Panama and was instrumental in helping me capture images of salp filtering meshes for the first time. He has been encouraging throughout the thesis process and has an amazing ability to work late into the night; I tried but failed to keep up with him. I am fortunate to have Peter Wiebe serve as chair of my defense. Like Larry, he has an enormous amount of perspective on the field of zooplankton ecology. I had an opportunity to work with him last summer (2008) and was amazed by his efficiency (he even walks the hallways quickly) and generosity with his time.

There are a number of other people at WHOI and elsewhere who enriched my experience. Erich Horgan was a constant presence in the lab, always willing to lend me a hand or piece of advice when I needed it, and with a smile. Annette Govindarajan shared insights into teaching undergraduates, which I tucked away for future reference and Dan Smith was a reliable presence during the night shift. I have enjoyed getting to know Kate Madin who has been supportive and also very patient in helping me write an Oceanus article. Much of the background for my low Reynolds number filtration chapter came from a class I took at MIT with Roman Stocker. Roman stayed involved long after the course ended and has been enormously helpful in guiding the mathematical aspects of that chapter. Norm Farr, optics guru (and senior engineer), was generous with his time and equipment and always willing to chat.

At various times, I had insightful conversations with Scott Gallagher, Cabell Davis, Carin Ashjian, Mark Baumgartner and Gareth Lawson about various aspects of my research. Terry Rioux kept me on top of all of my AAUS certifications. Rudi Rottenfusser from Zeiss microscopes was not only willing to lend me equipment but he also taught me a lot about microscopy. I had nothing but positive interactions with all of

the Biology Department administrators, especially Dianne Rossi, Erin Dupuis, Bonnie Cormier, Sue Tomeo, Marie Allen and Janis Umschlag. Julia Westwater, Marsha Gomes, Michelle McCafferty, Christine Charette and Valerie Caron from Academic Programs Office were super helpful and always responded quickly to any of my questions.

I would also like to thank all of the people that facilitated my work at the Liquid Jungle Lab (LJL) in Panama. Ellen Bailey not only took me sailing on Thursday afternoons, but also navigated the complications and miscommunications related to working in Panama with a bottomless store of patience. Luis Camilli, is not only competent lab director but also has a quirky sense of humor that I appreciated during my field visits. Dan Marin and Dave Kushner were the bluewater diving dream team – they were safe and efficient underwater and also game to take sunset hikes at the end of the day. Andrew Gray, Dave Sutherland, Emily Abbott, Holly Swift and Jane Lee also participated as divers during various trips. Gracias to all of the Panamanian staff at the lab – especially the boat drivers, Pacho and Benito. And, without J.P. Pigozzi, there wouldn't be an LJL.

I also want to thank all of my friends at WHOI who made life a lot more fun: Brosnahan, Carly, Breea, Dave, Erin, Emily, Casey, Joanna, Eoghan and Naomi. And, noontime soccer with the Woods Hooligans was seriously critical to my mind-body balance and I really enjoyed interacting with members of the Woods Hole community in that context.

My family members were ever supportive and full of good humor over my trips to Antarctica, Panama and Croatia to study these mysterious 'salps'.

Finally, I never would have guessed I would meet the love of my life, Dave Sutherland, during first year Biological Oceanography class. Not only was finding Dave the best thing that has ever happened to me but he also helped me with my fieldwork in Panama and with MATLAB code! Thank you Dave for your love, patience and companionship.

Funding to support my thesis research, tuition and stipend primarily came from two NSF grants (OPP-0338290 and OCE-0647723). I also received support from the WHOI Academic Programs Office in the form of a Fye teaching fellowship, an Ocean Ventures Fund award and assistance with tuition and travel to meetings and two summer courses. I received funds from MIT, WHOI Biology Department and Friday Harbor Labs for travel and tuition for a summer course at Friday Harbor Labs. Further research support came from the WHOI Ocean Life Institute and the Journal of Experimental Biology.

Contents

1.	Background	11
1.1	Salp life history and ecology.....	11
1.2	Morphology and movement.....	13
1.3	Suspension feeding by salps.....	15
1.4	Filtration mechanics.....	16
1.5	Study site.....	19
1.6	Research questions.....	20
1.7	General approach.....	21
2.	A comparison of filtration rates of pelagic tunicates using kinematic measurements	23
2.1	Abstract.....	23
2.2	Introduction.....	24
2.3	Methods.....	27
2.3.1	Data collection.....	27
2.3.2	Determination of kinematics and filtration rate.....	28
2.3.3	Comparison to other methods.....	29
2.4	Results.....	30
2.4.1	Individual body kinematics.....	30
2.4.2	Patterns in body kinematics and flow rate.....	33
2.4.3	Comparison with results from other methods.....	33
2.5	Discussion.....	36
2.5.1	Morphology, kinematic trade-offs and filtration rates.....	36
2.5.2	Comparison with other methods and broader applications.....	38
2.5.3	Optimized filtration.....	41

3.	Jet wake structure and swimming performance of pelagic tunicates	43
3.1	Abstract.....	43
3.2	Introduction.....	44
3.3	Methods.....	46
3.3.1	Specimen collection and observation.....	46
3.3.2	<i>In situ</i> dye visualization and laboratory PIV of salp jet wakes.....	46
3.3.3	Calculation of swimming performance variables.....	48
3.4	Results.....	49
3.4.1	Structure of propulsive jet wakes.....	49
3.4.2	Kinematic swimming parameters.....	52
3.5	Discussion.....	56
3.5.1	Aspects of salp jet wake structure.....	56
3.5.2	Swimming morphology, kinematics and performance.....	58
3.5.3	Ecological and evolutionary context for swimming patterns.....	60
4.	Filtration of submicrometer particles by pelagic tunicates	63
4.1	Abstract.....	63
4.2	Introduction.....	64
4.3	Methods.....	67
4.3.1	Collection of specimens.....	67
4.3.2	Parameter measurements.....	67
4.3.3	Low Reynolds number particle capture model.....	68
4.3.4	Particle capture experiments.....	71
4.4	Results.....	72
4.4.1	Mesh dimensions and particle speeds.....	72
4.4.2	Model predictions.....	73
4.4.3	Feeding experiments.....	76

4.5	Discussion.....	77
4.5.1	Model parameters.....	77
4.5.2	Limitations of model.....	79
4.5.3	Importance of submicron particles for salps.....	79
4.5.4	Impact of salps on marine ecosystems.....	80
5.	Conclusions	83
5.1	Thesis summary.....	83
5.2	Co-evolved swimming and feeding traits.....	84
5.2.1	<i>Pegea confoederata</i>	85
5.2.2	<i>Weelia cylindrica</i>	86
5.2.3	<i>Cyclosalpa</i> species.....	86
5.2.4	Paradox of the plankton.....	87
5.3	Future applications.....	88
5.3.1	Biogenic mixing.....	88
5.3.2	Coordinated swimming.....	89
5.3.3	Optimized filtration.....	90
6.	References	91

Chapter 1

Background

1.1 Salp life history and ecology

Salps are common gelatinous holoplankters in shelf and oceanic waters. They swim by jet propulsion, drawing water through incurrent and excurrent siphons at opposite ends of the body. Muscle bands encircling the cylindrical body drive a pulsed jet that propels the animal forward and also creates a feeding and respiratory current. Like other tunicates, salps use a fine mucous filter to remove a wide range of particles, including bacteria and phytoplankton, from the water column. The filter fills most of the barrel shaped body and is continually being generated, and then rolled up as a food strand that is conveyed to the esophagus. Salps achieve higher rates of filtering and efficiently retain smaller particles ($1\text{ }\mu\text{m}$ – 1 mm) than most other planktonic grazers (Madin and Deibel 1998). Salps therefore play a key part in pelagic ecosystems, particularly when they form dense swarms (Alldredge and Madin 1982). Due to their efficient removal of small particles from surface waters, salps are capable of packaging and exporting primary production to deeper waters, thus influencing biogeochemical cycling (Madin 1982, Madin et al. 2006).

Salps have a two part lifecycle composed of asexual, solitary individuals and sexual chains of aggregates. Asexual, solitary forms called oozoids give rise to smaller pseudo-colonial chains of identical blastozoids. There are tens to hundreds of sexually reproducing individuals in each chain and chains can be tens of meters long. Cross-fertilization normally does not occur within chains because individuals are protogynous hermaphrodites that change from females to males in approximate synchrony (Godeaux et al. 1998). Each individual broods a single embryo, or in a few species several embryos, which becomes a solitary budding individual.

Salps are most abundant in oceanic, warm water but some are found in temperate waters and in the Southern Ocean. They occur from surface to depths in excess of 1000 m and some are vertical migrators (Franqueville 1971, Wiebe et al. 1979). There is considerable variability in the morphology of individuals and the architecture of aggregate forms and this diversity in form is accompanied by variations in swimming behaviors (Madin 1990). The alternation of generations and short generation times, on the order of days to weeks, allows for rapid population growth when conditions are favorable. Populations in temperate and cold waters along continental shelves are known to periodically reach bloom proportions that extend for hundreds of kilometers (e. g. Madin et al. 2006). Given this range of habitats, we can expect that salps have developed a variety of morphological, behavioral and mechanical strategies for success in a variety of environments. On an evolutionary scale, morphological traits that relate to particular swimming and feeding mechanisms can be selected on the basis of the biological and physical environment. Although there are only 47 species of salps, many of them are cosmopolitan and overlapping in distribution. The co-occurrence of species with fundamentally similar, non-selective feeding mechanisms in a seemingly homogenous environment raises the question of what selective factors have led to speciation. Specific patterns of resource exploitation driven by morphology and behavior may have co-evolved in salps allowing for their co-existence.

1.2 Morphology and movement

Pumping water by salps fills the dual role of locomotion and filter feeding. This sets up a trade-off between two key processes and allows for a variety of lifestyles ranging from forms that can maximize particle flux through the filtering mesh to forms that can maximize locomotory capacity. Salps do show a range of swimming styles based on speeds, pulse rates, diel behavior and degree of musculature. Some of these distinct swimming styles are driven by morphology and the arrangement of individuals into chains. Fast swimming forms have higher pulse rates and streamlined, linear morphologies, and some migrate 100s of meters over diel cycles. One might expect that fast swimming forms have a lower cost of locomotion, traverse more volume in the horizontal and vertical dimensions and can potentially take better advantage of patches of increased food availability. Slower swimming forms tend to have slower pulse rates and less hydrodynamic forms. One might predict that slower forms cover less area but are more efficient at straining particles from the immediate environs. Both strategies are effective and allow different forms to partition a similar food resource.

The arrangement of blastozooids into chains differs strikingly among groups of salps and these differences are important for locomotion. Chain architectures can be described by six basic patterns: transverse, cluster, whorl, helical, oblique and linear (Madin 1990). The simplest form, found in *Pegea* spp., is the transverse chain. Salps are arranged side by side in a double row so that the oral siphons are all in a single plane and the atrial siphons are in a different, parallel plane. The most streamlined architecture, found in *Salpa* spp., is the linear chain. The blastozooids lie end to end with central axes parallel to the chain axis. In this configuration, the frontal surface area is minimized, thereby limiting the amount of drag experienced by a swimming chain. Each arrangement likely results in trade-offs between maximizing flux through the filtering meshes and optimizing locomotion.

Movement and filter feeding by salps is accomplished by pumping water into the oral aperture, through the pharyngeal and atrial chambers and out the atrial siphon (Madin 1974). In the process of pumping, food particles are strained through a mucous

net that occupies the pharyngeal chamber. During a pulse cycle, the oral siphon closes and circular muscle bands are contracted to eject water out the atrial siphon and propel the animal forward. When the muscles relax and the atrial siphon is closed, the body expands due to the resilience of the tunic, and water is drawn into the oral siphon to fill the body cavity. The result is a pulsing jet that produces cyclical changes in swimming velocity, or unsteady swimming. Salps are the only jet propelled creatures that have opposing anterior and posterior openings, allowing for unidirectional flow and forward and reverse swimming. Stimulation of one end of a chain results in acceleration or a coordinated reversal in swimming direction.

Jet propulsion has arisen in a variety of marine pelagic organisms including squid, siphonophores and medusae. Relative to other swimming modes, jet propulsion is considered an inefficient means of locomotion, which may explain why it is not more common (Alexander 2003, Biewener 2003). However, among the jet-propelled creatures, it has been suggested that salp swimming is the most economical (Bone and Trueman 1983). A pulsed jet, as opposed to continuous jet emission, may improve hydrodynamic efficiency because the wake rolls up into a series of vortex rings that interact to create additional thrust (Dabiri et al. 2005, Madin 1990, Daniel 1985, Weihs 1977). Previous measurements (Madin 1990) of the ratio of jet ring radii to jet core (b/ϵ) and the radius of ring spacing to ring radius (a/b) for a range of salp sizes and species confirmed that pulsed jets are hydrodynamically advantageous for salps. Another argument for the existence of jet propulsion in salps may be that it arose in part as a mechanism for creating filtering flows and not solely for transport. In cnidarian hydromedusae, the wakes generated by swimming motions create distinct feeding currents that directly relate to foraging preferences (Colin and Costello 2002, Colin et al. 2003). Similarly, flow patterns generated by swimming salps likely vary with morphology and swimming motions and result in differences in feeding performance.

Swimming by salps can also be considered in the context of an optimization theory of locomotion called constructal theory (Bejan and Marden 2006). The theory posits that convergences in functional characteristics of locomotion (e.g. an insect wing

and a bird wing) can be explained by the tendency of systems to evolve in such a way that flow through the system is optimized and energy expenditure is minimized. Therefore there are certain general design goals for optimized flow. This theory of flow optimization could apply to both locomotion and filtration but how resources are divided between these two essential processes generates the possibility for variation in the group. The morphology and behavior of salps makes them particularly appropriate models with which to examine this theory of flow optimization.

1.3 Suspension feeding by salps

Tunicates (or Urochordates) are suspension feeders that use various types of mucous filters to trap plankton and detritus. In contrast to other tunicates that produce a feeding current by ciliary action, salps produce unidirectional flow by rhythmically contracting muscle bands. As a salp swims, seawater and associated food particles are continually being filtered through a mucous mesh that fills the mostly hollow body. Fluid enters the pharynx through the oral aperture, particles are entrained on the mesh and then conveyed to the esophagus and gut. The mucous filter is produced within the endostyle, which is a ventral, longitudinal groove, and conveyed by cilia dorsally towards the peripharyngeal bands at the front end of the animal. The filter is attached to the dorsal gill bar, where the mucous sheet is continuously rolled into a food strand that moves posteriorly towards the esophagus. The net fills much of the pharyngeal cavity and resembles a bag-like plankton net. Unlike other ascidians, the net is not supported by a branchial basket and is probably maintained by water pressure.

The function of the endostyle and mucous filter in salps was first described 130 years ago by Fol (1876). Fol observed that the endostyle produced a mucous web that he was able to visualize with carmine particles in *Thalia democratica*. Fedele (1933) later detailed the anatomy and mechanics of ingestion in several species including *Thalia democratica*, *Cyclosalpa pinnata*, *Salpa maxima* and *Pegea confoederata*. He described 'slow' and 'fast' feeding modes with different levels of mucus production (Madin and Deibel 1998). This notion persisted until *in situ* observations (Madin 1974) showed that

‘slow’ feeding was a laboratory artifact. Recently, the secretion and deployment of the filter from the endostyle was examined in greater detail using scanning microscopy (Bone et al. 2000). This study provided insight into the production of the filter within the endostyle but a complete understanding of the way in which the filter is deployed and maintained would require work with live specimens.

In a natural setting, the filtering mesh appears to be in place almost all the time (Madin 1974) but may detach during reverse swimming (Bone et al. 1991). Under laboratory conditions or when particle densities are high, the net can become clogged and break. The net is then expelled through the oral siphon by rapid reverse swimming. Continued exposure to high particulates clogs the esophagus and prevents the animal from feeding (Harbison et al. 1986). This may explain the absence of most species of salps in near-shore regions where particulate levels are high. When the feeding process is interrupted, a new filter is produced within several minutes (Madin 1974). My observations of nets stained with carmine particles suggest that the filtering mesh is fully constructed within the endostyle before it is deployed. Deployment of a new net is rapid and appears to be aided by pulses of water that expand the net to fill the body, but details of this process are yet to be described.

1.4 Filtration mechanics

An understanding of filtration efficiency and particle selectivity of salps requires an understanding of the fluid mechanics at the level of the filtering mesh. Variables important for filtering include the volume of water and associated particles moving through the filter, the surface area of the filter and the pore size of the filtering mesh. By definition, suspension feeding is the concentration of particles from the surrounding medium by some type of filtration mechanism (Jorgensen 1983). This mode of feeding allows salps to survive and grow large in areas where food particles are relatively small and dilute.

Understanding of biological filters advanced with the application of engineering principles to filtration mechanics (Rubenstein and Koehl 1977). In addition to simple

sieving, capture mechanisms relevant to marine filter feeders include direct interception, inertial impaction, gravitational deposition and diffusional deposition. Using models set up in running water, Silvester (1983) showed that diffusional deposition and inertial impaction were negligible for particles smaller than 0.3 μm and larger than 50 μm respectively but these particle ranges are probably not ecologically relevant for salps. Shimeta and Jumars (1991) published an in depth modeling analysis that considered particle concentrations, velocity, particle size and filter element size, among other variables. They emphasized the distinction between using rate and efficiency as the dependent variables when predicting optimization schemes. These conceptual models of particle capture by suspension feeders can explain observed feeding patterns when accurate measurements of fluid structure local to the feeding structure and filter measurements are available.

Clearance rates and particle size retention efficiencies measured among salps (summarized by Madin and Deibel 1998) suggest a range of salp filter morphologies in terms of relative surface area, spacing of fibers and fiber diameter. In experiments with polystyrene beads, particles less than 1 μm were retained with low efficiency and cells larger than 4 μm were retained with 50-100% efficiency in five species studied (Kremer and Madin 1992). Harbison and McAlister (1979) reported some variability in retention efficiencies of three species of *Cyclosalpa* but all particles above 4 μm were retained with 100% efficiency. The authors concluded that differences in the lower particle size ranges were the result of differences in animal size. A feeding study in the Mid-Atlantic bight region using naturally occurring food particles suggested prey selection is dictated by mechanical constraints (Vargas and Madin 2004). *S. cylindrica* ingested larger prey such as dinoflagellates, *C. affinis* ingested smaller nanoflagellates and *T. democratica* ingested a combination of prey types. Comparisons between filter mesh measurements and particle size retention estimates will provide further insight into the mode of filtering that dominates at the level of the filtering apparatus.

The factors that are important for filtration performance include flux through the mesh and particle retention efficiency. Reynolds numbers based on salp size and overall

swimming speed are between 150 and 6000 for solitary salps. However, suspension feeding near the filtering apparatus of salps (Madin 1990) and ascidians (Jorgensen 1983) is characterized by considerably smaller Re on the order of 10^{-4} , indicating that viscous forces dominate particle filtration within the organism. Suspension feeding is the capture of particles in viscous, Stokes flow. Slight changes in viscosity will have substantial consequences for filtration rate and particle retention. Intuitively, decreasing the pore size seems like a good way to capture more particles. However, decreasing pore size increases the pressure drop thereby increasing the likelihood of damaging the filter and driving up the energetic cost of pumping fluid through the filter. The number of particles captured on the net will also be a function of the environmental particle concentration and size distribution.

Previously, the filtering meshes of several species of tunicates have been examined using scanning electron microscopy (SEM) and transmission electron microscopy (TEM) (summarized in Bone et al. 2003). The results from these studies have provided images of the filters as well as measurements of the spacing and thickness of the filter strands (Table 1.1). The filter has a square mesh in the endostyle but the mesh becomes rectangular after it has been deployed. A likely explanation is that the water pressure produced during the jet cycle stretches the elastic mesh more in one dimension. Particle retention measurements do not align closely with measured mesh dimensions. This could be due to experimental artifacts or the mechanics of filtration. The techniques used to visualize the nets require drying and extensive processing and the shrinkage that occurs during preparation is difficult to estimate (Bone et al. 1991). Mesh size data from prior studies are based on small sample sizes from two or three species and the methodologies varied (Table 1.1). The mesh size may fluctuate with location in the pharynx or with the phase of the jet cycle due to changes in water pressure. Finally, particles may be captured in ways other than simple sieving (Rubenstein and Koehl 1977, Shimeta and Jumars 1991). Additional measurements of filtering mesh pore sizes from a variety of species and from different parts of the mesh are necessary to resolve the mechanics of filtering at the mesh and to make comparisons among co-occurring species.

Table 1.1. Salp filter mesh measurements. Modified from Bone et al. 2003.

Species	Filter location	Method	Mesh spacing (μm)	Filament thickness (nm)	Source
<i>Salpa fusiformis</i>	Endostyle	SEM	1.3 x 1.3	200 x 200	Bone et al. 2000
<i>Pegea confoederata</i>	Pharynx	SEM	0.7 x 4.0	100 x 50	Bone et al. 1991
<i>Thalia democratica</i>	Pharynx	TEM	0.9 x 0.9	30 - 40	Bone et al. 2003
<i>S. fusiformis</i> or <i>Pegea socia</i>	Fecal pellets	SEM	0.3 x 5.4		Silver & Bruland 1981

1.5 Study site

The Liquid Jungle Lab (LJL) is an ideal research station for the study of salp swimming behavior both *in situ* and in the laboratory. The station is located on the island of Canales de Tierra off the Pacific coast of the Veraguas province of Panama, approximately 250 km from Panama City (7° 50' N, 81° 35' W). The lab is privately owned, and operated in cooperation with the Smithsonian Tropical Research Institute and the Woods Hole Oceanographic Institution. Lab facilities include biology and chemistry dry labs, a wet lab with a running seawater system, diving locker and boats and a library and conference room. Labs are air-conditioned and the entire station is equipped with wireless internet. There are dormitory accommodations, an on-site doctor and all meals are provided (see website at <http://www.liquidjunglelab.com/>).

Data-collection visits to the site during the dry season (January – March) between 2006 and 2009 confirmed that salps and other oceanic plankton are reliably present along the shelf region near the Island of Canales de Tierra within a one hour boat trip. Salps generally require collection from a research vessel, but this site provided an unusual opportunity for cost efficient and productive research because salps are common and can be maintained and studied from a shore-based laboratory with running seawater.

With the exception of Yount's work (1954), there is a lack of studies on the distribution and ecology of salps in the tropical Pacific (Madin and Swanberg 1984).

This study provided documentation of salp distributions and *in situ* plankton research in a relatively unexplored region.

1.6 Research questions

In order to understand the ecology of salps and, particularly how species can co-exist in similar environments, we must know something about swimming and feeding capabilities. The data presented here was collected at the Liquid Jungle Lab where salps were available for *in situ* work and collection and covered a range of scales to obtain a complete picture of the behaviors and mechanisms responsible for niche partitioning.

Through my thesis research, I sought to answer the following questions:

- How do flow patterns created by salps vary according to morphology and swimming motions and how do those patterns relate to swimming and feeding capabilities?
- How does the feeding mechanism influence selection and ingestion of food particles?
- How do filtering parameters relate to filtration efficiency?

This work also yielded insight into larger scale questions, including:

- Salps exhibit a range of morphologies and swimming modes. Do flows produced by planktonic organisms translate into unique foraging strategies?
- Both swimming and feeding are achieved by salps during jet propulsion. Does the optimization of locomotory performance occur at a cost to filtration performance and vice versa?
- How does form and function of salps align with phylogenetic relationships and what does this tell us about historical outcomes of various designs?
- Salps and other holoplanktonic grazers share the same three-dimensional environment. Do differences in morphologies and behaviors translate into specialization on a particular food resource (or, alternatively, have plankters arrived at multiple strategies for consuming a common resource)?

- Is salp design and movement consistent with theories of optimized locomotion systems? Does the dual role of swimming and feeding during jet propulsion result in deviations from optimal design characteristics?

1.7 General Approach

The aim of this project was to assess the adaptive advantage of distinct morphologies and swimming behaviors by salps in terms of feeding success and selectivity using laboratory and field experiments. *Salpa cylindrica*, a fast-swimming, streamlined chain, *Pegea confoederata*, a slower swimming chain, and *Cyclosalpa* spp., a slower swimming whorl, were the focus of these studies because they were sighted frequently during field visits and represent a range of salp swimming modes. Other species were incorporated when they were present. The study of salps and other fragile gelatinous organisms requires specialized methodologies. Behaviors are best studied in the organism's natural environment (Hamner et al. 1975) but more precise measurements can be made in the laboratory using diver-collected animals. *In situ* observations were conducted from a small boat using blue water SCUBA techniques (Haddock and Heine 2005). Salps used for laboratory work were hand-collected by divers in jars, maintained in jars or aquarium tanks and used for experiments within 12 hours of capture.

Chapter 2

A comparison of filtration rates among pelagic tunicates using kinematic measurements

2.1 Abstract

Salps have higher filtration rates than most other holoplankton, and are capable of packaging and exporting primary production from surface waters. A method of kinematic analysis was employed to accurately measure salp feeding rates. The data were then used to explain how diverse body morphologies and swimming motions among species and lifecycle stages influence salp feeding performance. I selected five species, representing a range of morphologies and swimming styles, and used digitized outlines from video frames to measure body-shape change during a pulse cycle. Time-varying body volume was then calculated from the digitized salp outlines to estimate the amount of fluid passing through the filtering mesh. This non-invasive method produced higher feeding rates than other methods and revealed that body volume, pulse frequency and degree of contraction are important factors for determining volume filtered. Each species possessed a unique combination of these three characteristics that resulted in comparable filtration (range: 0.44 - 15.33 ml s⁻¹) and normalized filtration rates (range: 0.13 - 1.06 s⁻¹) across species. The convergence of different species with diverse morphologies on similar normalized filtration suggests a tendency towards a flow optimum.

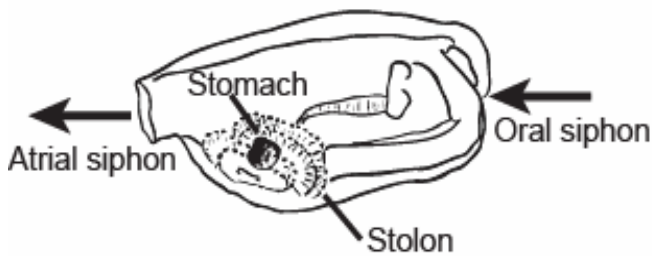
2.2 Introduction

Salps, or pelagic tunicates, are common gelatinous holoplankton in oceanic waters that occur from the surface to depths in excess of 1000 m. They swim by jet propulsion, drawing water in through the oral siphon and using muscle bands encircling the cylindrical body to eject water from the atrial siphon (Fig. 2.1a). The resulting pulsed jet propels the animal forward and also creates a feeding and respiratory current. Like other tunicates, salps use a fine mucus mesh to filter a wide range of particles, including bacteria and phytoplankton. During swimming, seawater and associated food particles are constantly being filtered through the mucous filter, which fills much of the body and is continually being generated, and then rolled up as a food strand that is conveyed to the esophagus (Madin 1974). Salps achieve higher rates of filtering and efficiently retain smaller particles (1 μm – 1 mm) than most other planktonic grazers (Madin and Deibel 1998) and therefore play a key part in pelagic ecosystems, particularly when they form dense swarms (Alldredge and Madin 1982). Due to their efficient removal of small particles from surface waters, salps are capable of packaging and exporting primary production to deeper waters, thus influencing biogeochemical cycling (Madin 1982, Madin et al. 2006, Phillips et al. 2009). Some species are vertical migrators, accelerating the transport of fecal material and biomass to deeper water.

Salps have a two part lifecycle composed of asexual, solitary individuals (oozoids) and sexual chains of aggregates (blastozooids). There is considerable variability in the morphology of individuals and the architecture of aggregate forms and this diversity in form is accompanied by variations in swimming behaviors (Madin 1990). Chain architectures can be described by six basic patterns: transverse, cluster, whorl, helical, oblique and linear (Madin 1990). The simplest form, represented by *Pegea confoederata* in Fig. 2.1b, is the transverse chain. Individual blastozooids are arranged side by side in a double row so that the oral siphons are all in a single plane and the atrial siphons are in a different, parallel plane. The most streamlined architecture, represented by *Weelia (Salpa) cylindrica*, is the linear chain (Fig. 2.1d). The blastozooids lie end to end with central axes parallel to the chain axis. I hypothesized that each morphology and

chain arrangement results in trade-offs between maximizing flux through the filtering meshes and optimizing locomotion.

A. *Pegea confoederata* solitary



B. *Pegea confoederata* aggregate



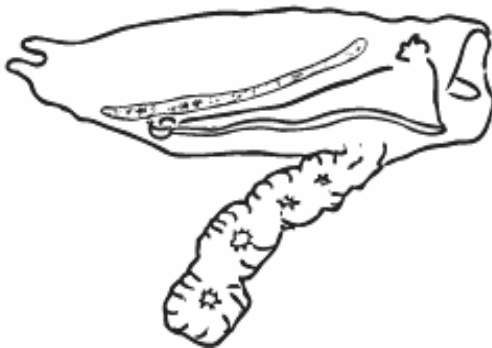
C. *Weelia (Salpa) cylindrica* solitary



D. *Weelia (Salpa) cylindrica* aggregate



E. *Cyclosalpa affinis* solitary



F. *Cyclosalpa sewelli* aggregate



1 cm

Fig. 2.1. Range of morphologies among solitary (A, C, E) and aggregate (B, D, E) salps from this study. Arrows show direction of water flow. Scale for all drawings at lower right.

During a pulse cycle, the buccal aperture closes and circular muscle bands are contracted to eject water out the atrial siphon and propel the animal forward. When the muscles relax and the atrial siphon is closed, the body expands due to the resilience of the tunic, and water is drawn into the oral siphon to fill the body cavity. It is plausible that this mechanism of jet propulsion in salps arose in part as a mechanism for creating filtering flows and not solely for transport. In cnidarian hydromedusae, the wakes generated by swimming motions create distinct feeding currents that directly relate to foraging preferences (Colin and Costello 2002, Colin et al. 2003). Similarly, I wanted to examine whether flows generated by swimming salps vary with morphology and swimming motions and result in differences in feeding performance.

Feeding rates of salps have previously been measured using a variety of methods, including gut pigment measurements, defecation rates and particle depletion rates (reviewed by Madin and Kremer 1995). Each of these methods confers advantages and disadvantages but all require at least some aspect of confinement, which leads to an underestimate of filtration rate. Salps are delicate and only survive for short periods of time in the laboratory (Madin 1974). Therefore, it is optimal to make measurements of swimming, feeding, and metabolism in the field. As an alternative method of measuring feeding, several investigators have measured internal body volume and then multiplied by pulse frequency to estimate the volume of seawater passing through the swimming salp (Anderson 1985, Bone et al. 1991, Madin and Kremer 1995). These estimates assume that 100% of the body volume is expelled during a pulse have mostly been used as a basis for comparison to other methods. In squid, however, more sophisticated body outline measurements have been used to estimate volume flow in a jet propelled organism (Anderson and Demont 2000).

Here I present an *in situ* method of kinematic analysis to measure change in body volume during a pulse cycle. The resulting volume flow rates are a measure of how much fluid and associated food particles pass through the filtering mesh and provide a metric of the upper limit of filtration. Filtration capability can then be directly compared between species. It is worthwhile to make a distinction between the different units of

feeding measurements. Filtration rate, synonymous with volume flow rate, refers to the volume of seawater and associated food particles passing through a feeding filter per unit time. Clearance rate measures a volume of seawater from which particles have been completely removed. If particles are removed with 100% efficiency, filtration rate and clearance rate are equal.

The work presented here is part of a larger study examining the trade-offs between filtration and jet propulsion among species of pelagic tunicates. The focus of the present study was to accurately measure filtration rates *in situ* in order to 1) determine an upper limit on salp filtration rate and 2) examine the role of form and function in salp feeding among species and lifecycle stages. Given the important role salps play in cycling of organic material and their potential to remove production from surface waters, accurate field estimates of filtration rates are critical to estimating their ecological impact.

2.3 Methods

2.3.1 Data collection

Five species of solitary and aggregate salps, *Pegea confoederata*, *Weelia* (*Salpa*) *Cylindrica*, *Cyclosalpa affinis*, *Cyclosalpa sewelli* and, *Cyclosalpa polae*, were studied in April 2007, January 2008 and January 2009 at the Liquid Jungle Lab on the Pacific coast of Panama (Fig. 2.1). The species selected represent the range of morphologies and swimming styles among salps. In all experiments, a Sony HDR-HC7 high definition camcorder (1440x1080 pixels, 29.97 fps) was used. Bluewater diving techniques were used for observation and collection (Hamner 1975, Haddock and Heine 2005). Divers videotaped salps *in situ* using an Amphibico Dive Buddy housing and High-Intensity Discharge 10 watt light to illuminate the animals and improve contrast. A camera framer with an attached plastic ruler provided scale and helped the videographer keep the study subject in the field of view.

Additional animals were hand-collected in 800 ml plastic jars by divers and videotaped in the laboratory within 6 hours of collection. Salps were transported and maintained in jars at field temperatures (26-28° C) until the time of filming. Before

filming, individuals were gently transferred to an acrylic tank containing seawater from the collection site and allowed to acclimate for several minutes. The tank was side lit to provide contrast and a 1 cm grid taped to the inside of the tank provided scale.

2.3.2 Determination of kinematics and filtration rate

Selected video clips when salps were swimming straight, parallel to the camera lens, and in the field of view for one or more pulse cycles were converted from Mini DV into digital files using Vegas Movie Studio editing software (Sony). Salp body length was measured from the oral siphon to the atrial siphon at the beginning and end of each swimming sequence to ensure the body maintained the same distance from the lens during the sequence. At each time step, the outline of the salp was digitized by manually selecting points around the perimeter of the body using MATLAB (MathWorks™). Though manually digitizing the salp outline was time consuming, contrast between the salp and the background was not sufficient to use an automated edge detection method.

Volume was estimated from the two dimensional salp outline using the shell method of integration, where discrete radii spanning from the body central axis to the outer edge of the body are rotated 360 degrees. Volumes of the upper and lower half of the salp were estimated individually and summed to get a more accurate estimate of volume, as presented in Equation 1.1:

$$V = 0.5\pi \int_0^L ([R_{upper}(x)]^2 + [R_{lower}(x)]^2) dx \quad (2.1)$$

where L is the length of the salp, R_{upper} and R_{lower} are radii at position x along the central axis, L . An assumption of this two-dimensional method is that compression is equal in the dorso-ventral and lateral dimensions. The volume at each time step was plotted for each individual swimming salp. A mean pulse frequency, f_{pulse} , for each salp was calculated using Equation 2.2:

$$f_{pulse} = 1/T_{pulse} \quad (2.2)$$

where T_{pulse} is the mean time interval between two volume maxima (or minima) and represents the time it takes for a single pulse cycle. Volume flow rate, Q , was calculated using Equation 2.3:

$$Q = \frac{\bar{V}_{\text{max}} - \bar{V}_{\text{min}}}{\bar{P}_{\text{time}}} \quad (2.3)$$

where \bar{V}_{max} is the mean maximum volume and \bar{V}_{min} is the mean minimum volume. The degree of compression, C , or how much fluid was ejected relative to the maximum volume, was calculated following Equation 2.4:

$$C = \frac{\bar{V}_{\text{max}} - \bar{V}_{\text{min}}}{\bar{V}_{\text{max}}} \quad (2.4)$$

Normalized volume flow rate was calculated by dividing by the mean body volume for each individual, allowing for direct comparison between individuals and species of different sizes. Note that the average salp volume includes both the internal volume and the body of the salp so these measurements cannot be directly compared to internal salp volumes reported elsewhere in the literature.

Kinematic volume flow rate data from individuals were combined to examine filtration rate, degree of contraction and pulse frequency among species as a function of body size and to determine how species-specific morphology and kinematics influence filtration rate.

2.3.3 Comparison to other methods

To evaluate this method relative to other methods, filtration rates of one species from this study, *P. confederata*, were compared to published clearance rates obtained using gut pigment, defecation rate and particle depletion rate methods. *P. confederata* was chosen to do this comparison because this species survives longer in containment than most other salp species and has been the subject of several feeding studies (Harbison and Gilmer 1976, Madin and Cetta 1984, Madin and Kremer 1995).

2.4 Results

2.4.1 Individual body kinematics

Outlines of the body as the salp goes from a maximum to a minimum volume illustrate the extent to which body shape changes, as well as areas where shape change is most concentrated (Fig. 2.2). In all species, contraction of muscle bands is most pronounced towards the anterior and posterior ends but there are individual differences in the percent of the body volume that is expelled. In most individuals, the posterior end appears most expanded when the salp volume is at a minimum. This is due to the widening of the atrial siphon during fluid expulsion. In most cases, the rest of the body appears only slightly contracted at a minimum volume but slight differences in the two-dimensional outline correspond with relatively larger differences in volume.

Change in body volume over several pulse cycles are shown for individual salps in Fig. 2.3. An increase in volume corresponds with water entering the oral siphon and a decrease in volume corresponds with water ejecting from the atrial siphon. Among the solitary salps, the slow-pulsing *C. affinis* (0.63 Hz) has the highest percent volume change per pulse (27 %), the fast-pulsing *W. cylindrica* (2.04 Hz) has a more modest change (18 %) and the moderately fast-pulsing *P. confoederata* (1.72 Hz) the lowest change in volume (11 %). Compared to solitary stages of the same genus, the aggregate stage salps examined have higher pulse frequencies and higher percent changes in volume. The slow-pulsing *C. sewelli* (1.16 Hz) has a high percent volume change per pulse (31 %), the fast-pulsing *W. cylindrica* (2.1 Hz) has a slightly lower change (28 %) and the moderately fast-pulsing *P. confoederata* (2.78 Hz) had the lowest volume change (22 %).

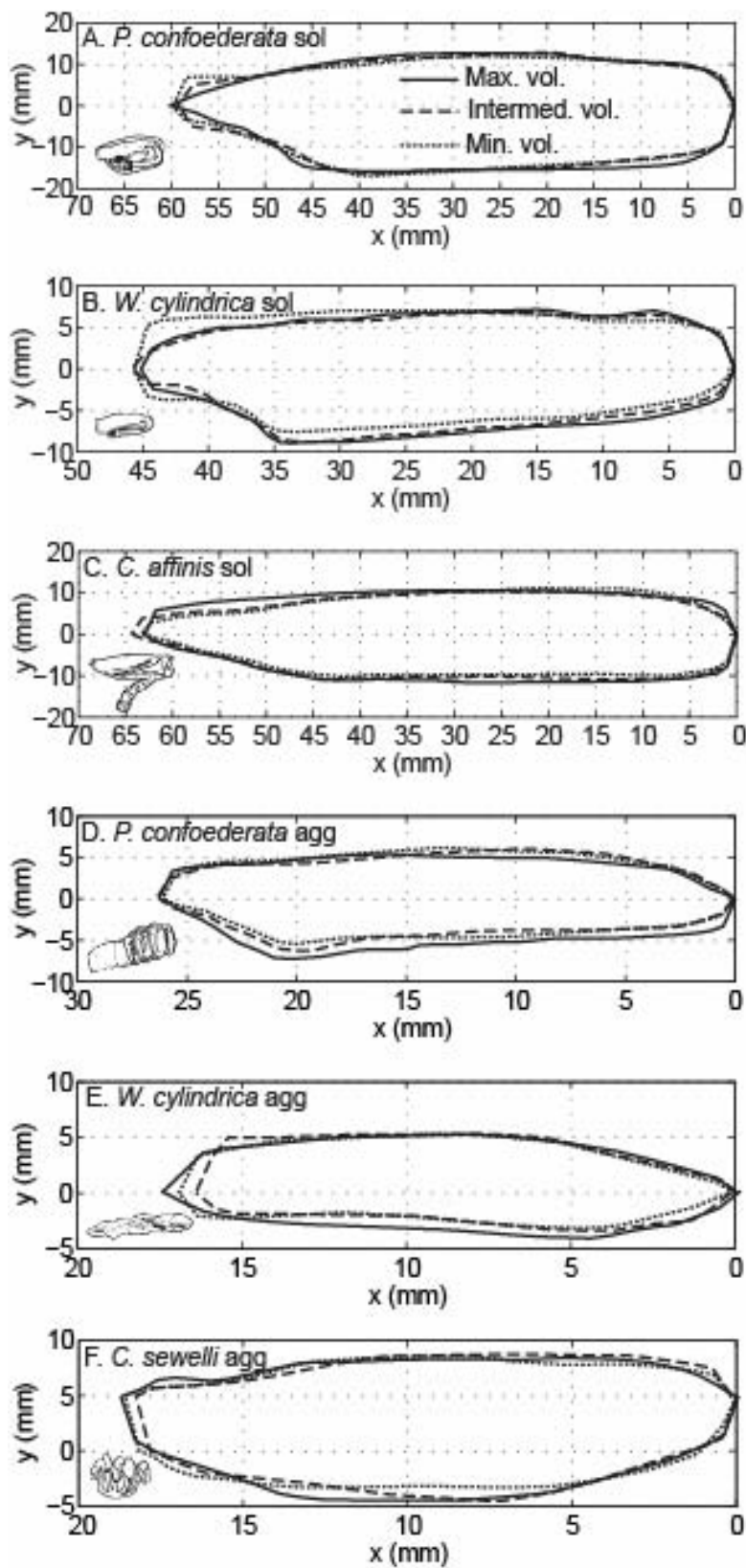


Fig. 2.2. Representative salp outlines from digitized video frames indicating body shape and size as volume decreases from a maximum to a minimum. Anterior end of salp faces to the right in each outline.

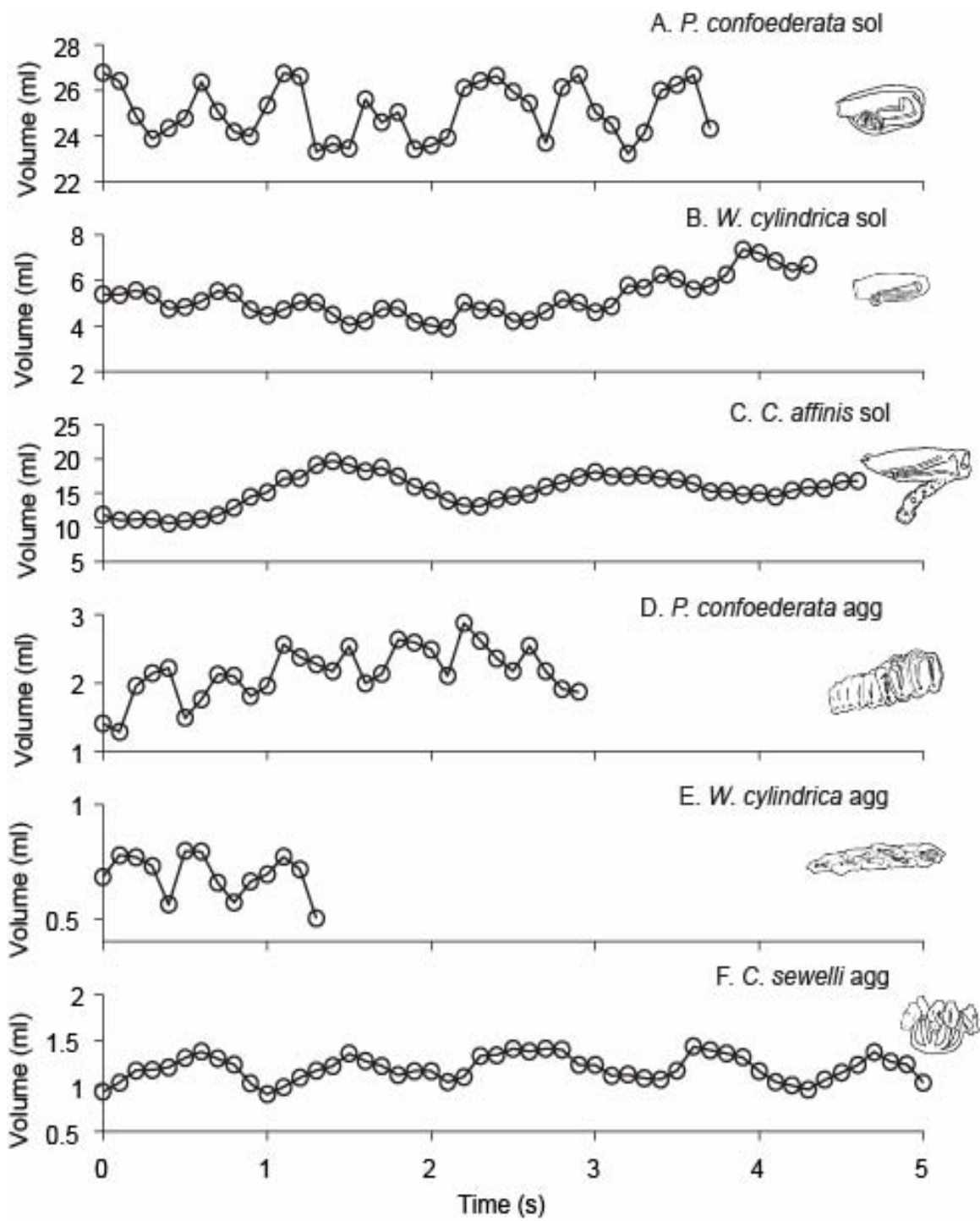


Fig. 2.3. Time varying body volumes of individual solitary (A-C) and aggregate (D-F) salps. Aggregate volumes are from one individual in chain.

2.4.2 Patterns in body kinematics and flow rate

Kinematic profile data from all individuals ($n = 55$) were combined to examine filtration rate and pulse frequency among species as a function of length and body volume (Table 2.1). Of the total measurements, 85% ($n = 47$) were collected in the field and 15% ($n = 8$) were collected in tanks. Pulse frequencies decreased with increasing length for all species (Fig. 2.4; Pearson Product Moment Correlation, $r = -0.395$, $p = 0.003$) and field and tank pulse frequencies were not significantly different (ANCOVA, length as covariate, $F_{1,51} = 0.26$, $p = 0.61$). Salps with higher body volumes (V) had higher filtration rates (F) (Fig. 2.5; Linear Regression, $\log(F+1) = 0.266 + 0.0297*V$, $r^2 = 0.76$, $p < 0.001$). When filtration rate was normalized to account for differences in body volume, pulse frequency (f_{pulse}) and body contraction (C) were good predictors of normalized filtration rate (F_n) (Fig. 2. 6; Multiple regression, $\arcsin \sqrt{F_n} = -0.290 + (0.289*P) + (2.153*C)$, $r^2 = 0.87$, $F_{2,51} = 172.93$, $p < 0.001$). When comparing among species, there were differences in three characteristics between different species and life cycle stages: volume, pulse frequency and degree of body compression (Table 2.1). A unique combination of these three characteristics within each species resulted in similar filtration rates and normalized filtration rates among all species (Table 2.1). *P. confederata* solitaries filtered the highest volumes but they were only significantly different from *C. sewelli* aggregates, which had the lowest filtration rates. *W. cylindrica* aggregates had significantly higher normalized flow rates than all other species.

2.4.3 Comparison with results from other methods

Feeding rate results for *P. confederata* from this study were compared to results from previous studies. A comparison of raw data from this study and regression lines from data using three other methods show that this study produced the highest values, setting an upper limit on measured feeding rates (Fig. 2.7; Harbison and Gilmer 1976, Madin and Kremer 1995). Feeding rates from gut pigment studies, a primarily *in situ* technique, were higher than the lab-based defecation rate and particle depletion studies. Data from Madin and Kremer (1995) were reported as clearance rates and data from

Table 2.1 Morphometric and kinematic data of salp species studied (mean \pm SEM). ANOVA comparisons of volume filtered and normalized volume filtered are presented at bottom of columns. Means labeled with same letters are not significantly different (Tukey's test, $p < 0.05$).

	N	Length (mm)	Body volume (ml)	Pulse frequency (Hz)	% volume change	Vol. filtered (ml s ⁻¹)	Normalized vol. filtered (s ⁻¹)
Solitary salps							
<i>Pegea confoederata</i>	12	47.0 \pm 3.8	15.8 \pm 3.0	1.8 \pm 0.1	17.8 \pm 1.8	5.8 \pm 1.3 ^a	0.34 \pm 0.03 ^a
<i>Weelia cylindrica</i>	18	38.4 \pm 1.3	5.0 \pm 0.4	2.1 \pm 0.1	17.2 \pm 0.9	2.0 \pm 0.2 ^{ac}	0.41 \pm 0.03 ^a
<i>Cyclosalpa affinis</i>	4	62.5 \pm 6.0	15.9 \pm 3.5	0.67 \pm 0.1	30.3 \pm 1.3	4.2 \pm 1.1 ^{ac}	0.24 \pm 0.03 ^a
<i>Cyclosalpa sewelli</i>	4	30.5 \pm 6.0	5.2 \pm 3.4	1.4 \pm 0.2	28.9 \pm 2.9	3.6 \pm 3.0 ^{ac}	0.47 \pm 0.12 ^a
<i>Cyclosalpa polae</i>	2	64.0 \pm 1.0	16.5 \pm 0.3	1.0 \pm 0.6	23.5 \pm 5.5	3.9 \pm 1.8 ^{ac}	0.24 \pm 0.11 ^a
Aggregate salps							
<i>Pegea confoederata</i>	8	29.3 \pm 3.3	6.9 \pm 2.6	2.1 \pm 0.1	18.3 \pm 1.6	2.5 \pm 0.8 ^{ac}	0.43 \pm 0.06 ^a
<i>Weelia cylindrica</i>	2	18.5 \pm 2.5	1.0 \pm 0.3	2.5 \pm 0.4	29.9 \pm 1.8	1.0 \pm 0.5 ^{ac}	0.86 \pm 0.21 ^b
<i>Cyclosalpa sewelli</i>	5	19.0 \pm 1.7	1.6 \pm 0.3	1.6 \pm 0.2	24.6 \pm 2.4	0.6 \pm 0.1 ^{bc}	0.44 \pm 0.05 ^a
						F _{7,47} = 2.68	F _{7,47} = 4.81
						p = 0.02	p < 0.001

Harbison and Gilmer (1976), as well as this study are filtration rates. Therefore, comparing directly between results requires an assumption that particles were retained with 100% efficiency in filtration rate studies.

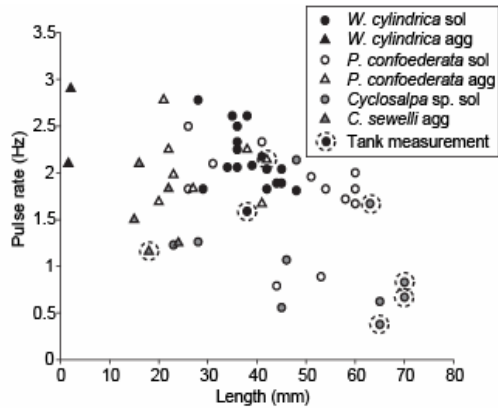


Fig. 2.4. Relationship between salp body length and pulse frequency. Tank measurements are circled to distinguish them from field measurements.

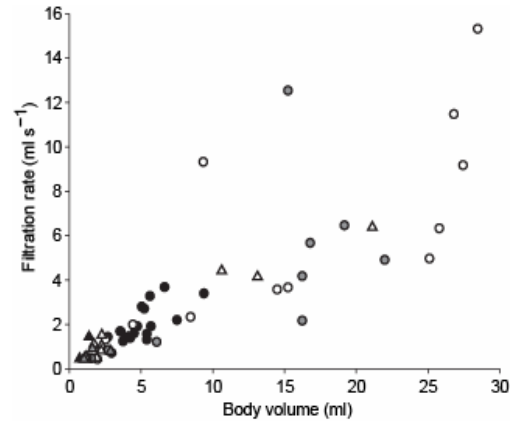


Fig. 2.5. Relationship between salp body length and filtration rate. Symbols are the same as Fig. 2.4.

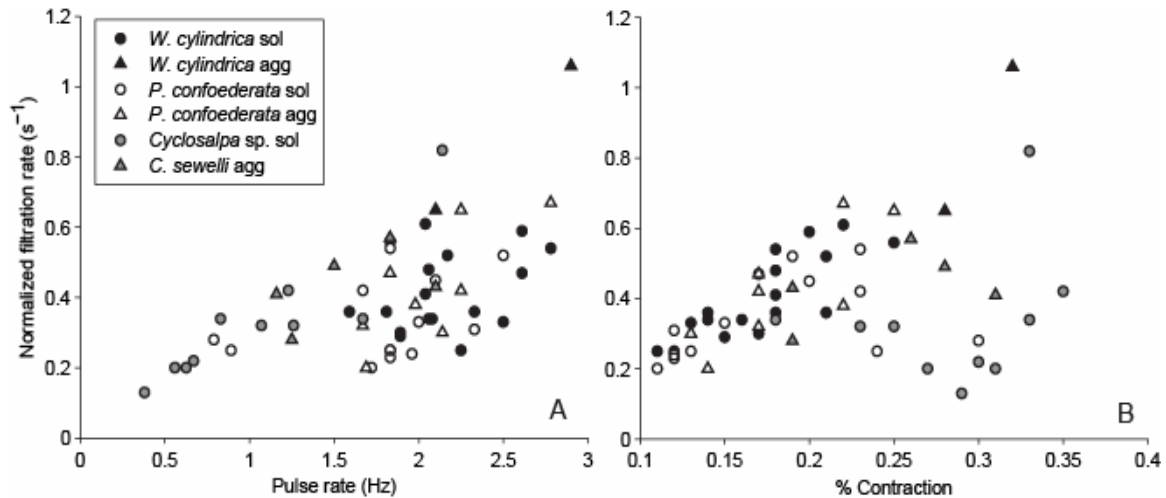


Fig. 2.6. Influence of A) salp pulse frequency and B) percent contraction on filtration normalized to body volume.

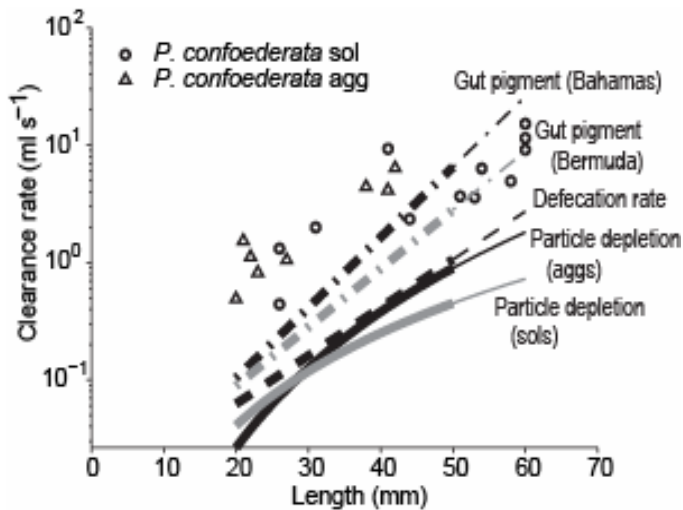


Fig. 2.7. Comparison of *P. confoederata* clearance rate methods from this study (open symbols) with other studies (regression lines). Regression lines are extended (thin lines) to facilitate visual comparisons. Gut pigment and defecation rate data from Madin and Kremer (1995). Particle depletion data from Harbison and Gilmer (1976).

2.5 Discussion

2.5.1 Morphology, kinematic trade-offs and filtration rates

Salp species exhibit a range of morphologies and swimming kinematics that play an important role in feeding rates. An examination of the kinematics of swimming at the individual level shows that each species has a unique morphology associated with a particular swimming pattern and manner of changing shape during a pulse (Figs. 2.1, 2.2, 2.3). In all species, most of the alteration in shape during a pulse is at the anterior and posterior apertures of the animal due to articulations at the oral and atrial siphons (Fig. 2.2). Body size, pulse frequency and degree of compression are important determinants of the amount of fluid a salp can filter (Figs. 2.5, 2.6). Our results suggest that while each species possesses a unique combination of these three characteristics, normalized filtration rates are comparable across species (Table 2.1). For example, *Cyclosalpa* species have slow pulse frequencies but compensate with pronounced contraction during pulses that expels a greater volume of fluid compared to the other species studied. Conversely, *W. cylindrica* solitaires have high pulse frequencies but a shallow pulse that expels relatively little fluid. *W. cylindrica* aggregates present an exception to this pattern

of trade-offs among kinematic traits because they have the highest pulse frequencies *and* highest pulse compression resulting in a normalized volume filtered that is almost double any of the other species (Table 2.1). High pulse frequencies and pulse compression likely contribute to high swimming speeds among *W. cylindrica* and other *Salpa* species aggregates reported in other studies (Madin 1990, Nishikawa and Terazaki 1994).

Several anatomical features of salps directly impact swimming and pumping capabilities and may help to explain differences in kinematics. The tunic, which surrounds the tube-like body, varies in stiffness and thickness (Hirose et al. 1999). During swimming, the muscle bands contract against the tunic to reduce the body volume and refilling is achieved due to elastic recoil of the tunic (Bone and Trueman 1983). Therefore, the physical properties of the tunic are important for pumping. *P. confoederata* solitaries and aggregates have particularly thick, stiff tunics which probably relates to shallow compressions (Table 2.1, Figs. 2.2, 2.3), due to the difficulty of compressing the test. Similarly, *W. cylindrica* solitaries have relatively stiff tests, though not quite as thick as those of *P. confoederata*, and correspondingly shallow compressions. On the other hand, *W. cylindrica* aggregates have relatively stiff tests (though slightly thinner than in solitaries) but their compressions are pronounced. As in *Salpa fusiformis* (Bone and Trueman 1983), lateral regions of the test are thin, possibly allowing for greater articulation at these points. Generally speaking, *Cyclosalpa* sp. solitaries and aggregates have thin, watery tests that cause these species to become flattened when they are removed from the water. The flexibility of the test allows for deeper compressions with each pulse. Because the tunic provides protection, much like an exoskeleton, having a flimsier body wall may improve pumping capabilities but could also confer increased vulnerability to predation. The number and arrangement of muscle bands as well as the number of muscle fibers, which are frequently used for taxonomic classification (e.g. Godeaux 1998), might also be expected to influence swimming capabilities but the relationship is less apparent.

2.5.2 Comparison with other methods and broader applications

The method of using video and kinematic analysis to measure salp feeding compares reasonably to other methods, though it produces consistently higher values (Fig. 2.7). Measured filtration rates of *P. confoederata* solitaries and aggregates from this study were 0.44 – 15.33 ml s⁻¹. Maximum measured clearance rate using particle depletion methods produced the lowest values, on the order of 1 ml s⁻¹ (Harbison and Gilmer 1976). The maximum measured clearance rate using gut pigment was slightly higher at ~1.7 ml s⁻¹ (Madin and Kremer 1995). Though not shown in Fig. 2.7, *P. confoederata* filtration rates determined from multiplying pumping rates by internal volume were higher than particle depletion and gut pigment measurements but were lower than measurements from this study (Madin and Kremer 1995). This was surprising because the measurements in Madin and Kremer (1995) were based on the assumption that the total internal volume is expelled, which would tend to overestimate filtration rate, since only a portion of the internal fluid is actually expelled. A closer comparison of the data revealed that the pulse frequencies in the Madin and Kremer study were much lower than those measured in the present study (by half or less), probably because they were tank measurements. The difference in results between the kinematic measurements and the simpler, pumping calculations underscores the importance of making accurate measurements of volume under natural, field conditions. Similar to the *P. confoederata* measurements, *W. cylindrica* and *Cyclosalpa* sp. feeding rates measured in this study were also higher than previous measurements obtained using other methods (Table 2.1, Madin and Deibel 1998). Though a range in feeding rates is probably in part due to differences in environmental parameters and individual behaviors, it is also due to measurement artifact. Of previously used methods, particle depletion involves the longest period of containment and therefore produces the lowest feeding rates. Gut pigment, on the other hand, involves the measurement of chlorophyll and its degradation products from guts of freshly collected salps. Gut pigment results are therefore consistently higher than more lab-intensive methods (Fig. 2.7, Madin and Kremer 1995). Kinematic measurements used in this study are less invasive than other methods, easily applied in the field and most accurately reflect natural feeding behaviors. These feeding

measurements represent the upper limit of filtration capability among salp species and allow for direct comparisons between salps with different morphologies and swimming kinematics. For aggregate forms, kinematic measurements may still occasionally underestimate volume flow rates. Bone and Trueman (1983) found that instantaneous velocities of individuals in an aggregate chain were smoother due to the coordinated swimming of individuals in the chain. Processing of additional fluid due to continuous forward swimming might produce even higher filtration rate than those presented here. A more general limitation of any filtration rate technique is that it indicates how much fluid is processed, but not how many food particles are removed. However, measurements of particle concentration, size spectra and retention rates could be used to extend this method and produce ingestion rates.

This non-invasive technique is particularly useful for active, fast-swimming species or fragile species because when observations are collected *in situ*, measured filtration rates capture typical feeding behavior. Moreover, certain species, including *W. cylindrica*, have been deemed “impossible” to maintain in captivity (Madin and Cetta 1984). To varying degrees, most salp species are easily damaged, swim slowly and/or erratically and don’t produce feeding nets when maintained in captivity. When all species were analyzed as a group, there was no significant difference between field and tank measurements in this study (results section). The similarity between field and tank measurements is likely due to careful collection and handling of specimens and very short periods of captivity. Looking at individual species however, the tank-measured *W. cylindrica* solitary had the lowest pulse frequencies of all *W. cylindrica* solitaires and the tank-measured *C. sewelli* aggregate had the lowest pulse frequencies of all *C. sewelli* aggregates (Fig. 2.4). Slower than normal pulse frequencies are an indicator of atypical behavior (personal observation).

Though feeding rate measurements will relate to the specific study and materials available, the kinematic method sets an upper limit on filtration capability and allows for direct comparisons of feeding rates among salp species, while also revealing particular functional aspects behind feeding efficiency. Similar *in situ* video analysis techniques

could also be adapted to non-invasively examine feeding among other fragile oceanic taxa. For instance, field measurements of appendicularian tail beat frequency and tail dimensions have already been successful in estimating clearance rates that agreed with laboratory studies (Bochdansky and Deibel 1999). In the broader oceanic context, kinematic measurements reaffirm that salps have some of the highest feeding rates among filter feeders with rates on the order of $1\text{-}10\text{ ml s}^{-1}$ (Table 2.1). Making accurate *in situ* measurements of salp grazing is critical to furthering our understanding of cycling and removal of primary production in oceanic surface waters.

Increasingly, kinematics and fluid mechanics techniques are being used to understand the functional underpinnings of zooplankton feeding. Since feeding rates of salps and other filter feeders have been compared previously (Alldredge and Madin 1982), here I will mention more recent zooplankton studies that used kinematics or fluid mechanics techniques. Units have been converted to ml s^{-1} to facilitate direct comparisons with results from this study. The study mentioned above used *in situ* measurements of tail beat frequency and tail dimensions and found that the appendicularian *Oikopleura vanhoeffeni* had filtration rates of 0.058 ml s^{-1} , about two orders of magnitude lower than salps (Bochdansky and Deibel 1999). Fluid velocity measurements of doliolids using videomicroscopy showed even lower filtration rates between 0.0002 ml s^{-1} (*Dolioletta gegenbauri* oozoid, Bone et al. 1997) and 0.001 ml s^{-1} (*Doliolum nationalis* phorozoid, Deibel and Paffenhöfer 1988). However, it is likely that confinement in a small container under the microscope resulted in lowered filtration rates. Flow rates through the appendages of the copepod *Temora longicornis* measured using quasi three dimensional Particle Image Velocimetry were between $0.0009\text{ - }0.003\text{ ml s}^{-1}$, similar to doliolids (van Duren et al. 2003). Copepods used in the study were cultured in the laboratory and then tethered during the study. The authors point out that tethering may actually lead to an overestimation of volume processed because the organism has to accelerate the fluid instead of moving through it. This discussion of other studies is by no means exhaustive but highlights some of the challenges with these types of measurements and reiterates the value of *in situ*, free-swimming measurements.

Furthermore, comparing results reveals that other zooplankton filter feed at rates are orders of magnitude less than kinematic measurements of salp filtration (0.44 – 15.33 ml s⁻¹).

2.5.3 Optimized filtration

The finding that salp species with different body shapes have very similar filtration rates can be considered in the context of an optimization theory called constructal theory (Bejan and Marden 2006). The theory posits that convergences in functional characteristics of locomotion can be explained by the tendency of systems to evolve in such a way that flow through the system is optimized and energy expenditure is minimized. Therefore there are certain general design goals for optimized flow. In the case of salp species, different morphologies and kinematics converge on similar normalized volume flow rates (Table 2.1) which also minimize energy costs. The higher normalized flow rates of *W. cylindrica* aggregates could be due to other ecological factors. Pumping fulfills a dual role of feeding and swimming, and *W. cylindrica* and *Salpa* species are fast swimming and sometimes diel vertical migrators (Madin et al. 1996). It may be that increased energy expenditure for feeding flows is a consequence of faster swimming. *Weelia cylindrica* has higher weight specific rates of oxygen consumption, carbon ingestion and ammonium excretion compared to most other species of salps (Madin and Deibel 1998). The energetic demands of high pulse frequencies might be balanced by higher rates of filtration and ingestion.

It has been suggested that all salp species are ‘ecological equivalents’, with little differentiation in diet, distribution, behavior or other parameters of their ecological niches (Yount 1954). The varied morphologies described here and elsewhere (Madin 1990) affect swimming performance and appear related to major adaptive strategies (i.e. migrator or not). Our observation that several species with different morphological and kinematic properties end up with similar net flow rates, suggests to us that the differences are important to other biological functions, such as reproduction, predator avoidance or life-history strategy, but that there is some optimum balance of flow rate and energy cost

that is most adaptive for the collection of food in the open ocean environment which is home to these species. It would be interesting to make the same observations on the small coastal species *Thalia democratica* to see if it has similar normalized flow rates.

In many ways, salps appear to be perfectly adapted to life in the limitless space of the open ocean water column. The flow of seawater through their bodies and filtering nets is their central interaction with this environment. Our results suggest optimization of this flow is achieved by different combinations of size, shape and behavior among several different species and generations of salps.

Chapter 3

Jet wake structure and swimming performance of pelagic tunicates

3.1 Abstract

Salps are barrel-shaped marine invertebrates that swim by jet propulsion. Morphological variations among species and life-cycle stages are accompanied by differences in swimming mode. The goal of this investigation was to compare propulsive jet wakes and swimming performance variables among morphologically distinct salp species (*Pegea confoederata*, *Weelia (Salpa) cylindrica*, *Cyclosalpa affinis*) and relate swimming patterns to ecological function. Using a combination of *in situ* dye visualization and particle image velocimetry (PIV) measurements, I described properties of the jet wake and swimming performance variables including thrust, drag and propulsive efficiency. Locomotion by all species investigated was achieved via vortex ring propulsion. I found that the slow-swimming *P. confoederata* produced the highest weight-specific thrust ($T = 53 \text{ N kg}^{-1}$) and swam with the highest whole-cycle propulsive efficiency ($\eta_{wc} = 55\%$). The fast-swimming *W. cylindrica* had the most streamlined body shape but produced an intermediate weight-specific thrust ($T = 30 \text{ N kg}^{-1}$) and swam with an intermediate whole-cycle propulsive efficiency ($\eta_{wc} = 52\%$). Weak swimming performance variables in the slow-swimming *C. affinis*, including the lowest weight-specific thrust ($T = 25 \text{ N kg}^{-1}$) and lowest whole-cycle propulsive efficiency ($\eta_{wc} = 52\%$), may be compensated by low energetic requirements. Swimming performance variables are considered in the context of ecological roles and evolutionary relationships.

3.2 Introduction

Salps are pelagic tunicates that swim by jet propulsion. A propulsive jet for locomotion is created by rhythmic compression of muscle bands encircling the barrel shaped body. Fluid enters the anterior oral siphon to fill the mostly hollow body of the salp. Next, the oral lips close and circular muscle bands contract, decreasing the volume of the jet chamber so that fluid is accelerated out of the anterior, atrial siphon (Fig. 3.1). By the end of the jet period, the atrial siphon is closed and the oral lips open to repeat the unsteady, rhythmic process. Though swimming by jet propulsion is employed by several other marine organisms including squid, medusae, and scallops, salps are unique in possessing incurrent and excurrent siphons on opposite ends of the body, allowing for unidirectional flow and reverse swimming during escape.

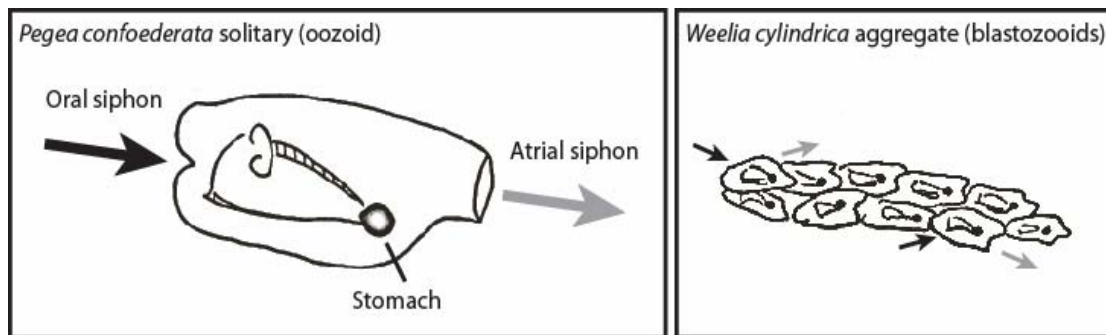


Fig. 3.1. Schematic illustration showing structures and fluid flow through siphons in a solitary *P. confoederata* and an aggregate *W. cylindrica*.

Among the approximately 40 species of salps, there are a range of body morphologies and swimming styles that likely relate to ecological roles of co-occurring species (Godeaux 1998, Madin 1990). Within each species, the salp life cycle is composed of two morphologically distinct stages; a solitary, asexually reproducing form (oozoid) buds off an aggregate, sexually reproducing form (blastozooid) comprised of tens to hundreds of identical individuals. Blastozooids in turn give rise to the next generation of oozoids. Beyond the individual anatomy of blastozooids and oozoids, the arrangement of individual blastozooids into aggregate chains is also unique between

species. Blastozooids are attached via plaques and communication between individuals allows for coordinated, though typically asynchronous, swimming and a coordinated escape response (Bone et al. 1980). Blastozooids are often asymmetrical, with atrial siphons at an angle relative to the axis of the chain. The range of body morphologies and chain architectures and associated swimming dynamics were described in detail by Madin (1990). Fast swimming salps are characterized by enhanced musculature, higher pulse frequencies and linear, streamlined chain structures compared to slower, surface oriented salps.

Studies of salp swimming kinematics are few, and investigations of the jet wake properties have been limited to a single species (Bone and Trueman 1983, Madin 1990). The goal of this study was to compare the propulsive jet wake structure and swimming performance among different species of salps with distinct morphologies. Comparative swimming performance among salps is of particular interest because swimming and feeding are achieved by the same pumping process. In the process of drawing fluid through the body of the salp during jet propulsion, fluid and associated particle pass through a mucous filter-feeding net. Particles between 0.1 and 1 μm , primarily phytoplankton, are captured by the net and conveyed to the gut (Madin and Deibel 1998). Therefore, a trade-off is established between these two fundamental activities.

In order to compare the kinematics and hydrodynamics of salp swimming, several species of salps representing a range of morphologies, chain architectures and swimming styles were investigated: *P. confoedertata*, *W. cylindrica*, *C. affinis*, *C. sewelli* and *C. quadriluminis*. First, the structure of propulsive jet wakes was characterized using *in situ* dye visualization and two-dimensional laboratory particle image velocimetry (PIV). Dye wake measurements provide a view of the full, ‘three-dimensional’ wake structure in the natural fluid environment and were used to verify that laboratory-based measurements were a reflection of normal swimming behavior. PIV techniques have been used to study the flow patterns around a variety of aquatic organisms (Stamhuis and Videler 1995), but this is the first application of the method to pelagic tunicate swimming. Second, kinematic and swimming performance variables were calculated from PIV video

sequences. Given that swimming by salp aggregates occurs in three-dimensional space and is therefore difficult to capture with a two-dimensional tool, the majority of the PIV data and kinematic variables focus on solitary forms.

3.3 Methods

3.3.1 Specimen collection and observation

Salps were collected and observed at the Liquid Jungle Lab off Pacific Coast of Panama, Veraguas province (7° 50' N, 81° 35' W) during January of 2007, 2008 and 2009. The species examined represented the range of morphology and swimming kinematics among salps and included, *P. confederata*, *W. cylindrica*, and *C. affinis*. Bluewater diving techniques were used for collection and field observations (Haddock and Heine 2005).

3.3.2 *In situ* dye visualization and laboratory PIV of salp jet wakes

Propulsive jet wakes of salps were visualized using two approaches: 1) fluorescein dye during night SCUBA dives and 2) PIV in the laboratory. SCUBA divers performed in situ wake flow visualizations, during night dives, using a Sony HDR-HC7 high definition camcorder (1440x1080 pixels, 30 fps) with an Amphibico Dive Buddy camcorder housing and a High-Intensity Discharge 10 watt light to illuminate the salp and dye structures. A plastic ruler placed in the field of view provided scale. Salps were approached slowly to avoid creating turbulence and fluorescein dye was ejected from a micropipette a few millimeters upstream of the oral siphon. In-focus frames that were not occluded by excess dye were selected to represent wake patterns.

Quantitative PIV data were recorded in the laboratory with salp specimens that were hand collected in 800 ml plastic jars by SCUBA divers and then maintained at field temperatures (26-28° C) (Fig. 3.2). Within 8 hours of collection, salps were transferred from jars into custom-built acrylic tanks filled with field-collected seawater seeded with 8-12 μm titanium dioxide particles. Tanks were 6-10 L in volume depending on the size

of the experimental animal. PIV allows for quantitative analysis of flow created by swimming animals in a two dimensional plane (Adrian 1991, Prasad 2000). The motion of small, reflective particles is measured by analyzing the positions of particles in sub-windows between successive frames. Particles were illuminated with a 300 mW, continuous green (532 nm) laser directed through a Powell lens (Lasiris) to produce a 1 mm-thick light sheet. The laser was positioned to one side of the tank with the camera parallel to the laser sheet. In some cases, a second 300 mW laser or a mirror was placed on the opposite side of the tank to improve illumination. The motions of the particles were imaged with a Sony HDR-HC7 high definition camcorder (1440x1080 pixels, 30 fps) and subsequently processed using LaVision DaVis 7.2 software. Image pairs were processed using a multi-pass, cross-correlation technique with a final interrogation sub-window of 32 x 32 pixels and an overlap of 16 pixels. The cross-correlation processing technique maps vectors based on the spatial shift of multiple particles between successive frames in a small area (McKenna and McGillis 2002). Resultant velocity vector fields were examined to identify swimming jets in which the salp and the atrial siphon remained in approximately the same lateral position for the duration of the jet.

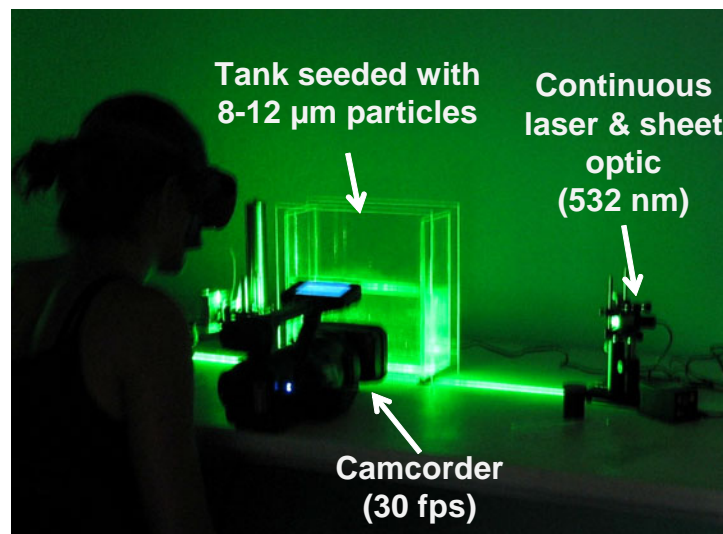


Fig. 3.2. Laboratory PIV configuration. Salps swam in a tank seeded with small, reflective particles. A laser sheet illuminated particles motions, which were recorded by a high definition camcorder.

Jet structure and velocity as well as body velocity were determined by analyzing sequences of images. Jet velocity was measured by taking a time-series of transects perpendicular to the jet, just aft of the atrial siphon. A mean jet velocity, u_m , and the maximum velocity, u_{max} , were calculated from individual transects. Since the values on either side of the jet profile approached zero, the mean jet velocity was not a reliable estimate of the true jet velocity. Therefore, the time average of the maximum jet velocity, u_{max} , over the entire jet period was used as the estimate of the jet velocity, \bar{u}_j . Because inspection of the PIV video clips revealed some streaking in the images, jet velocities were also calculated by measuring streak lengths from each image, u_s , to test the accuracy of the PIV velocity transects. Time averaged velocities from streak measurements, \bar{u}_s , were not significantly different from time averaged maximum jet velocities from PIV, \bar{u}_j (t-test, $t = -0.259$, $df = 22$, $p = 0.8$), therefore, \bar{u}_j was used for time-averaged jet velocity in all calculations. Since the PIV algorithm also tracks the high-contrast portions of the salp body, body velocity was calculated by taking a series of transects through a distinguishable landmark along body, usually the gut. The values were relatively constant across the transect, so the mean velocities at each transect, U , were averaged to produce a time-averaged body velocity, \bar{U} .

Morphometric measurements of body length, L , maximum body width, W , and maximum atrial siphon diameter, d , were obtained using ImageJ (<http://rsbweb.nih.gov/ij>). To adjust for size differences among salps species, swimming speed was converted to body length per time (\bar{U}/L). The relative streamlining of each salp species was estimated using the fineness ratio, the ratio of length to the width of a body, L/W (Vogel 1994).

3.3.3 Calculation of swimming performance variables

Morphometric and kinematic data were used to calculate jet thrust, drag and propulsive efficiency. All parameters were calculated in the steady sense, using time-averaged swimming parameters. Jet thrust, T , is the rate that an animal transfers momentum to the water (i.e. $F=ma$) and was calculated using the following equation:

$$T = \rho \bar{u}_j^2 A_j, \quad (3.1)$$

where ρ is seawater density (1021 kg m^{-3} at 28°C) and A_j is the maximum jet area determined from $\pi d^2/4$, where d is siphon diameter. Weight specific thrust, T_w , was also determined based on relationships between live length and carbon weight (Madin et al. 1981). Drag, D , was calculated using the following equation:

$$D = \rho \bar{U}^2 A_p C_d, \quad (3.2)$$

where A_p is the projected area. For fusiform objects like salps, it is appropriate to use $A_p = V^{2/3}$, where V is body volume (Vogel 2003). Body volumes were determined from relationships between salp length and body volume published in the literature (Madin et al. 1981, Madin and Purcell 1992). The drag coefficient, C_d , was calculated using a relationship with Reynolds number (Re), for $1 < Re < 500$ (Daniel 1983):

$$C_d = 24/Re^{0.7}, \quad (3.3)$$

where $Re = Ud/\nu$ and ν is kinematic viscosity ($1.05 \times 10^{-6} \text{ m}^2 \text{ s}^{-1}$). Slip, a measure of wasted energy, was calculated as $1 - \bar{U}/\bar{u}_j$. Propulsive efficiency was calculated in three ways: Froude propulsive efficiency, η_F , rocket motor propulsive efficiency, η_r , and whole-cycle propulsive efficiency, η_{wc} (Anderson and Demont 2000):

$$\eta_F = 2\bar{U}/(\bar{U} + \bar{u}_j), \quad (3.4)$$

$$\eta_r = 2\bar{U}\bar{u}_j/(\bar{U}^2 + \bar{u}_j^2), \quad (3.5)$$

$$\eta_{wc} = 2\bar{U}\bar{u}_j/(3\bar{U}^2 + \bar{u}_j^2). \quad (3.6)$$

Anderson and Demont (2000) examined the suitability of several equations of propulsive efficiency for squid swimming and concluded that during jetting, the equation for rocket motor propulsion was most appropriate. Rocket motor efficiency applies during periods of fluid output only, whereas Froude propulsive efficiency applies to simultaneous fluid intake and output, as in an airscrew. Neither equation accounts for losses due to intake and deceleration of a working fluid as occurs in squid and most other jet-propelled organisms. Therefore, Anderson and Demont (2000) derived equations for both squid whole-cycle propulsive efficiency (rear intake) and for scallop whole-cycle efficiency (forward intake) that account for losses during the refill period. The equation for scallops (Eq. 3.6), assumes the intake velocity to be very nearly the oncoming flow speed during

refill as the valves open- a sort of ‘ram refill’. This is a good assumption in salps, as well, where forward motion of the body would be expected to drive fluid into the body as the lips of the oral siphon open.

3.4 Results

3.4.1 Structure of propulsive jet wakes

In situ dye visualization showed the formation and evolution of dye wakes produced by salps swimming in the natural marine environment and PIV vector plots provided a more quantitative view of the jet structure in two dimensions. Both methods of flow visualization showed that in all species examined, forward swimming is accomplished by vortex ring propulsion. The jet can be described as a fully-pulsed jet, meaning there was a period of no flow separating pulses (Krueger et al. 2008). Fluid inside the body of the salp was accelerated as circular muscle bands contract and is ejected via the atrial siphon. The atrial siphon was circular in cross section at the beginning of the jet period and compressed to a horizontal slit by the end of the jet period (Fig. 3.3). Consecutive jets were spaced such that there was no evidence of interaction between vortex rings. Differences in the structure of the rings and trailing wakes corresponded to different swimming strategies among species and life history stages. Jet structures ranged from discrete vortex ring ‘puffs’ with no trailing jet to a small vortex ring and a long trailing jet.

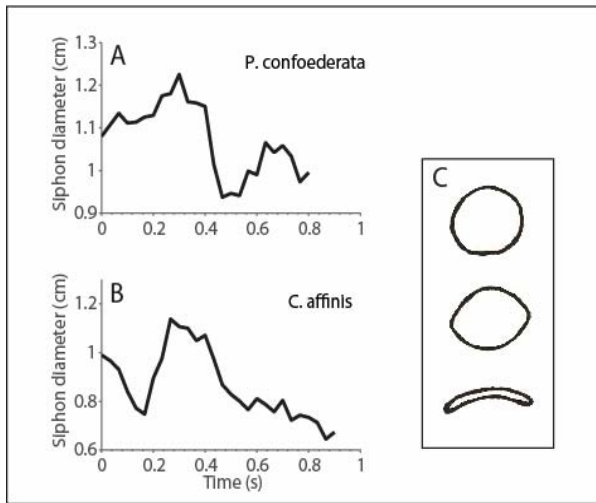


Fig. 3.3. Change in salp atrial siphon diameter d with time. (A) 63.3 mm-long *P. confoederata*, (B) 63.3 mm-long *C. affinis* and (C) cross section of *P. confoederata* atrial siphon over course of jet period sketched from salp swimming perpendicular to 1-mm thick laser sheet.

In the slow swimming *P. confoederata* solitaires (Figs. 3.3a, 3.4) and aggregates (Fig. 3.4b), the majority of the ejected fluid was entrained into a vortex ring with a low-volume trailing tail. Note that though there were only two individuals in the *P. confoederata* aggregate chain in Fig. 3.4b, there are often 10s to 100s of individuals in a chain. The pattern of classic, circular vortex rings and no trailing jet was particularly evident in the PIV vector plot (Fig. 3.5).

In the fast swimming *W. cylindrica* solitaires the jet period was short and there was a clear trailing wake with a small vortex ring, indicating that most of the ejected fluid remained in the trailing tail (Fig. 3.4c, 3.6). Compared to *W. cylindrica* solitaires, *W. cylindrica* aggregates also produced a small vortex ring but the flow in the trailing tail was more elongate and appeared quite laminar (Fig. 3.4d). Siphons are angled relative to the chain axis and therefore produce jets that propagate away from the axis of travel.

Among *Cyclosalpa* species, classic, spherical vortex rings *and* vortex rings with a large-volume trailing jet were observed. The solitary *C. affinis* individuals in Figs. 3.3e and 3.6 produced classic spherical vortex rings with no trailing jet. In other cases, however, jet flow became unstable and turbulent (personal observation from unpublished image sequences). In *C. sewelli* aggregates, the body volume was large relative to the siphon diameter and as the fluid was ejected, almost all of it was entrained into a vortex ring with no trailing jet (Fig. 3.4f). The individual *C. sewelli* in Fig. 3.4f has become

detached but aggregates of this species are typically in a wheel-shape with individuals joined via peduncles (resembling spokes) to a central attachment point (Fig. 2.1f). In both *C. sewelli* and *C. quadriluminis* aggregates, which also have a wheel-like arrangement, jets were angled away from the direction of travel (Fig. 3.4f, 3.8).

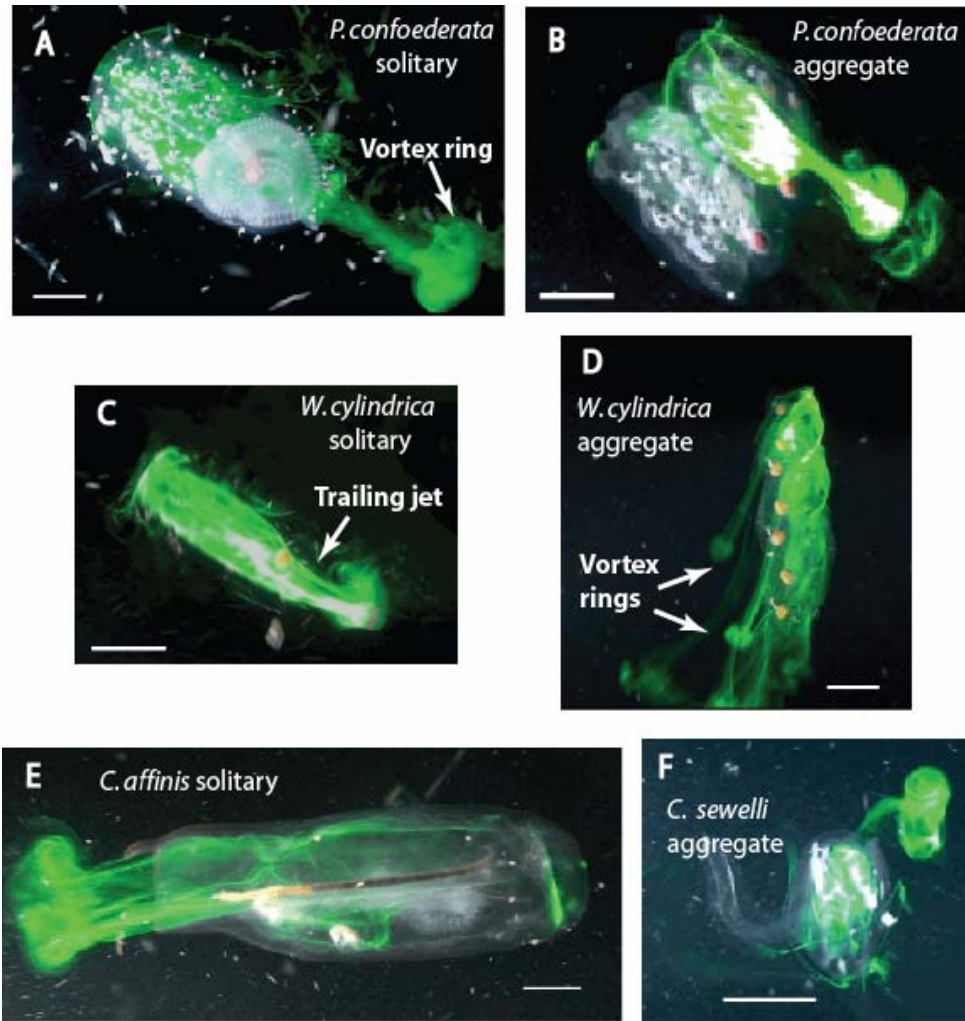


Fig. 3.4. *In situ* jet wake structures made visible with fluorescein dye. (A) *P. confoederata* solitary, (B) *P. confoederata* aggregate, (C) *W. cylindrica* solitary, (D) *W. cylindrica* aggregate, (E) *C. affinis* solitary and (F) *C. sewelli* aggregate. Scale bars are 1 cm.

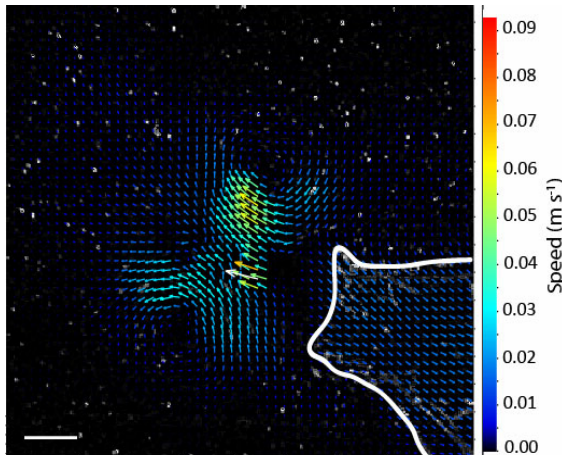


Fig. 3.5. Representative vector plot of a *P. confoederata* solitary jet wake showing circular vortex ring. Body outline sketched in white. Scale bar is 5 mm.

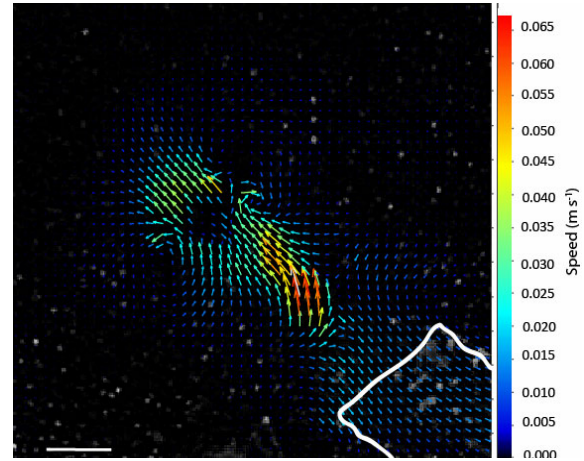


Fig. 3.6. Representative vector plot of a *W. cylindrica* solitary jet wake showing circular vortex ring and trailing jet. Body outline sketched in white. Scale bar is 5 mm.

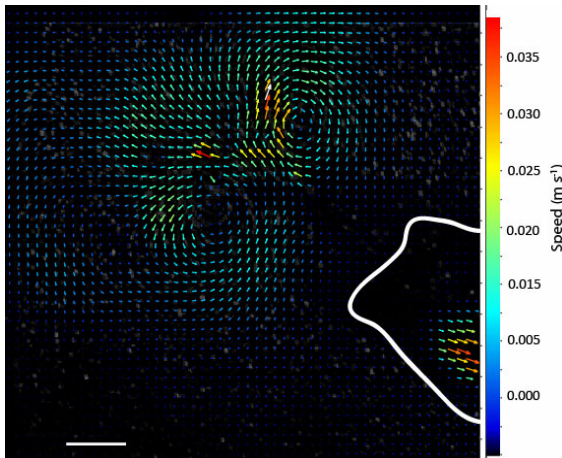


Fig. 3.7. Representative vector plot of a *C. affinis* solitary jet wake showing circular vortex ring. Body outline sketched in white. Scale bar is 5 mm.

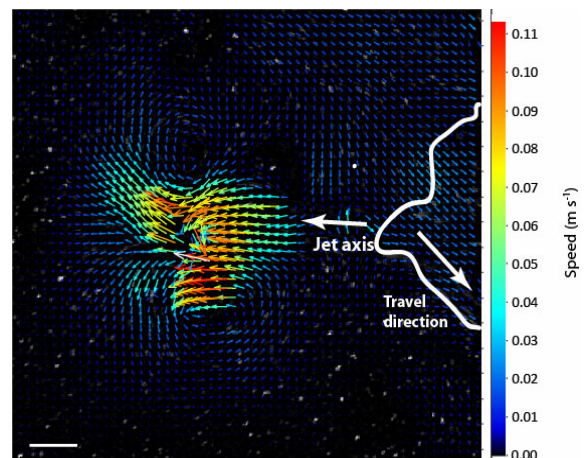


Fig. 3.8. Representative vector plot of a *C. quadriluminis* aggregate jet wake showing circular vortex ring. Body outline of jetting individual and neighboring blastozoid sketched in white. Scale bar is 5 mm.

3.4.2 Kinematic swimming parameters

Salp species vary in basic morphology and swimming kinematics. Time-varying jet velocity showed distinct patterns for *P. confoederata*, *W. cylindrica* and *C. affinis* solitaires (Fig. 3.9). Mean jet velocity in *P. confoederata* exhibited an initial increase in

velocity followed by a plateau and then a velocity spike towards the end of the jet period. In *W. cylindrica*, there was also an initial increase in jet velocity but then velocity continued to increase gradually to a maximum followed by a decline. In *C. affinis*, initial jet velocity was low and then gradually increased to a maximum followed by a relatively sharp decline. In all three species, the maximum velocity occurred about two-thirds of the way through the jet period.

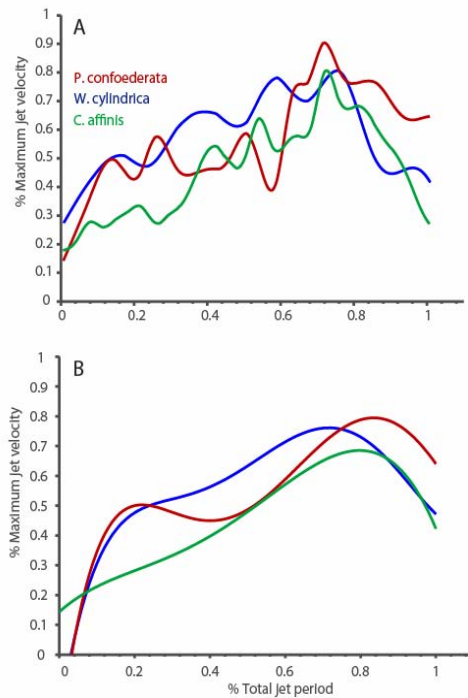


Fig. 3.9. (A) Mean jet velocity during jet period for *P. confoederata*, *W. cylindrica* and *C. affinis*. Each jet is normalized to the same duration and expressed as % of maximum velocity to allow for comparisons between species. N= 4 for each species. (B) Polynomial fits to curves plotted in (A).

Swimming kinematic data indicated that the fast-swimming *W. cylindrica* was the most streamlined, and exhibited the highest pulse frequencies and shortest jet period (Table 3.1). The slow-swimming *P. confoederata* was the least streamlined and had an intermediate pulse frequency and jet period length compared to the other two species. The relatively slow-swimming *C. affinis* had an intermediate degree of streamlining, the lowest pulse frequencies and longest jet period. For salp species in general, there were no clear patterns between swimming speed (Lengths s^{-1}) and jet speed or jet period (Fig. 3.10, b). Body speeds measured during the jet period were much lower than overall swimming speeds reported in the literature, suggesting that maximum body speeds

occurred after the end of the jet period (Table 3.1). When body speed was considered in terms of specific speed (body lengths s^{-1}), *P. confoederata* and *W. cylindrica* were comparable and *C. affinis* swam slightly slower (Table 3.1).

Table 3.1 Salp morphometric and kinematic variables. Values are means with ranges in parentheses.

	<i>Pegea confoederata</i>	<i>Weelia cylindrica</i>	<i>Cyclosalpa affinis</i>
Number of individuals	4	4	4
Length (mm)	50.8 (39.0- 60.3)	39.5 (36.0- 43.4)	64.1 (63.2- 65.0)
Swimming speed* (cm s^{-1})	4.1 (1.7- 5.6)	6.0 (2.5- 13.9)	4.8 (2.5- 5.9)
Pulse Frequency [§] (Hz)	1.5	2	0.8
Jet period (s)	0.52 (0.37- 0.80)	0.36 (0.2- 0.43)	0.69 (0.53- 0.93)
Fineness ratio	2.12 (1.92- 2.40)	2.59 (2.16- 2.96)	2.26 (1.90- 2.73)
Body speed (cm s^{-1})	1.68 (0.81- 2.22)	1.23 (0.85- 1.60)	1.72 (0.87- 3.11)
Body speed (Lengths s^{-1})	0.32 (0.21- 0.41)	0.31 (0.22- 0.41)	0.27 (0.14- 0.50)
Jet speed (cm s^{-1})	3.27 (2.03- 4.64)	3.34 (3.23- 4.25)	3.30 (2.52- 3.89)

* Data from Madin (1990).

§ Data are averaged from Madin (1990) and Chapter 2.

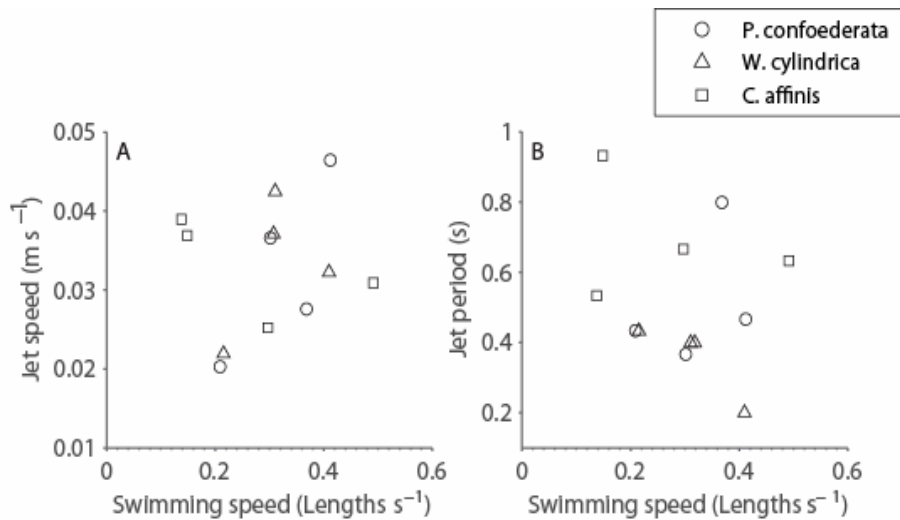


Fig. 3.10 (A) Jet speed, and (B) jet period as a function of specific swimming speed for *P. confoederata*, *W. cylindrica* and *C. affinis*.

There was no relationship between swimming speed and weight-specific thrust when all species were considered together (Fig. 3.11a), though *P. confoederata* exhibited substantially higher weight-specific thrust than the other two species (Table 3.2). Differences in drag were consistent with other swimming performance variables. The species with the lowest specific swimming speed and thrust, *C. affinis*, also experienced the highest drag (Tables 3.1, 3.2). Slip declined and efficiency increased with increasing swimming speed (Fig. 3.11b, c, d), indicating that swimming at higher speeds enhances performance. As expected, Froude and rocket motor propulsive efficiencies, which do not account for energy losses during refill, were higher than whole-cycle propulsive efficiency (Table 3.2). Though *C. affinis* had the lowest whole-cycle propulsive efficiency, *W. cylindrica* had the lowest Froude and rocket motor efficiencies. The maximum swimming efficiency by all three propulsive efficiency measures was achieved by *P. confoederata*.

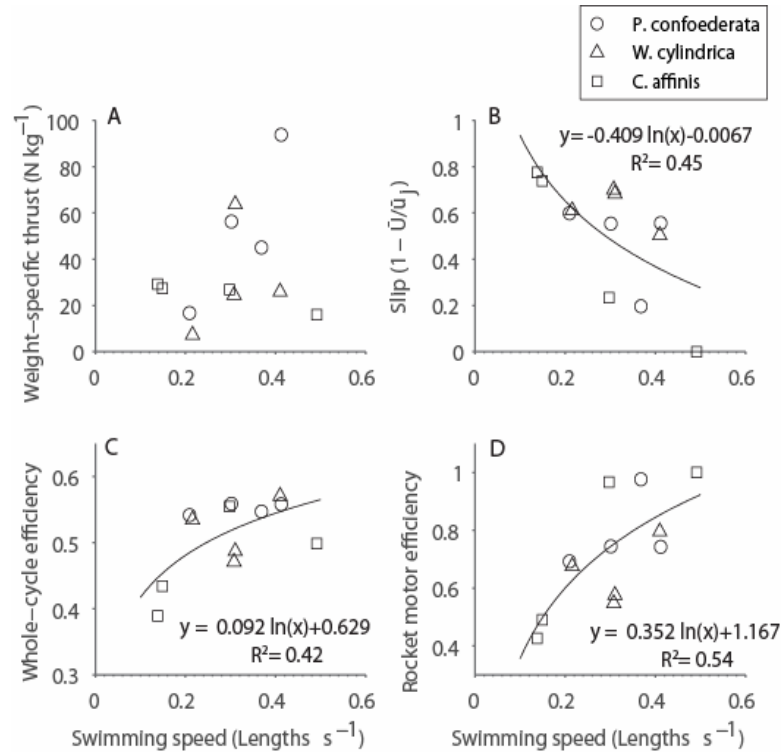


Fig. 3.11. (A) Weight-specific jet thrust, (B) slip ($1 - (\bar{U}/\bar{u}_j)$), (C) whole-cycle propulsive efficiency (Anderson and Demont 2000), and (D) rocket motor propulsive efficiency as a function of specific swimming speed for *P. confoederata*, *W. cylindrica* and *C. affinis*.

Table 3.2 Salp swimming performance variables. Values are means with ranges in parentheses.

	<i>Pegea confoederata</i>	<i>Weelia cylindrica</i>	<i>Cyclosalpa affinis</i>
Number of individuals	4	4	4
Thrust (N x 10 ⁵)	8.82 (2.05- 14.89)	5.27 (1.19- 12.44)	10.7 (6.69- 12.23)
Weight-specific Thrust (N kg ⁻¹)	53.0 (16.7- 93.9)	30.4 (24.5- 72.9)	24.9 (16.0- 29.2)
Drag (N x 10 ⁵)	1.50 (1.43- 5.84)	1.04 (0.70-1.41)	4.07 (1.19- 8.59)
Froude propulsive efficiency	0.67 (0.61- 0.89)	0.54 (0.48- 0.66)	0.66 (0.37- 1.00)
Rocket motor propulsive efficiency	0.78 (0.69- 0.98)	0.65 (0.55- 0.80)	0.72 (0.43- 1.00)
Whole-cycle propulsive efficiency	55.1 (54.1- 55.9)	51.6 (47.1- 57.1)	47.0 (38.9- 55.5)

3.5 Discussion

3.5.1 Aspects of salp jet wake structure

The findings presented here represent the first comparative study of salp jet wake structure and swimming performance. General aspects of salp jet propulsion in all species and life-history stages included: 1) fully pulsed jets, meaning there was a period of no flow between pulses, 2) production of vortex rings during each pulse (Figs. 3.3-7), and 3) an initial increase in siphon diameter followed by a decrease over the course of the jet period (Fig. 3.3). Based on an analytical model, Weihs (1977) showed that closely-spaced periodic jets result in substantial increases in thrust. More recent studies with squid and a mechanical pulsed-jet vehicle have confirmed a thrust benefit from pulsing compared to a continuous jet (Krueger et al. 2008). As a vortex ring forms, ambient fluid is accelerated and entrained in the growing ring. Variation in siphon diameter can delay pinch off of the ring from a trailing jet so that even more fluid is entrained in the vortex ring (Dabiri and Gharib 2005). Each of these features, characteristic of salp jet propulsion, were associated with the entrainment of additional, ambient fluid which leads to increased thrust (Dabiri 2009, Krueger et al. 2008).

Though vortex ring propulsion was common to all species in this study, diverse morphologies and swimming kinematics related to differences in swimming speed and

performance. Propulsion was achieved in *P. confoederata* solitaires and aggregates via classic vortex ring puffs (Figs. 3.3a, b, 3.4) whereas *W. cylindrica* solitaires and aggregates employ vortex rings with a trailing jet (Fig 3.3c, d, 3.6, 3.7). Among *Cyclosalpa* species, a combination of isolated vortex rings and vortex rings with trailing wakes were used (Fig. 3.4e, f, 3.7, 3.8). Each species also employed a characteristic velocity profile during jet formation that may relate to propulsive strategy (Fig. 3.11). The wake structures observed among salps are similar to the two jet modes described in the squid, *Loliguncula brevis*, throughout ontogeny (Bartol et al. 2009). In jet mode I, which was associated with higher propulsive efficiency, all of the fluid ejected from the siphon was entrained into an isolated vortex ring. In jet mode II, which was associated with greater thrust but lower propulsive efficiency, part of the fluid was entrained into a leading vortex ring but the remainder formed a long trailing jet. The finding that isolated vortex rings were more efficient than vortex rings with trailing jets is consistent with studies using mechanical pulsed jets (Krueger et al. 2008). Though Bartol et al. (2009) used a different propulsive efficiency equation, my calculations show that *P. confoederata*, which consistently produced isolated vortex rings (i.e. jet mode I), also had the highest Froude and rocket motor propulsive efficiency (Table 3.2). Conversely, *W. cylindrica* produced leading vortex rings with a trailing jet, and had the lowest Froude and rocket motor propulsive efficiency (Table 3.2). In contrast with squids, leading vortex rings with a trailing jet (i.e. jet mode II) observed in *W. cylindrica* and occasionally in *C. affinis* were not associated with higher thrust in salps (Table 3.2).

Pulsed jets can be considered in the context of recent work on optimal vortex ring propulsion. Studies using mechanically generated jets have shown that thrust is maximized when the jet length-to-diameter ratio (L/D), called the formation number (F), lies between 3.6 and 4.5 (Gharib et al. 1998). Above this optimum range, the leading vortex ring becomes disconnected or ‘pinched off’ and is followed by a trailing jet. Recent work with jet-propelled organisms has revealed that the formation numbers at which discrete vortex rings are formed may differ from this optimum. Pipe jet experiments and studies with jet-propelled organisms have shown that the optimum F can

be affected by at least two phenomena: 1) background co-flow can lower the optimum F due to early pinch-off or inhibition of vortex rings, leading to elongated jets with weak or absent vortex rings (Anderson and Grosenbaugh 2005) and 2) variation in jet diameter and/or jet velocity can delay pinch off (Dabiri and Gharib 2005). The jets of steadily swimming squid, which always experience co-flow due to flow past the squid occur at formation numbers of $F = 5.5- 61.8$ (adult *Loligo pealei*) and $F = 3.23- 23.19$ (juvenile and adult *Loliguncula brevis*) (Anderson and Grosenbaugh 2005, Bartol et al. 2009). These ranges extend well above 3.6- 4.5 and since co-flow reduces optimum F , squid jet events are frequently elongated plugs of fluid rather than discrete vortex rings (Anderson and Grosenbaugh 2005). Variation in jet diameter by *Nemiopsis bachei*, a cnidarian jellyfish species that swims by jet propulsion, led to a maximum F of around 8, and vortex ring pinch-off never occurred (Dabiri et al. 2006). Certain features of salp jet propulsion, including a variable atrial siphon diameter (Fig. 3.3) and fluid acceleration for the first two thirds of the jet period (Fig. 3.9), may lead to vortex formation numbers greater than the optimum range. Further work will be needed to resolve aspects of vortex formation and structure among salps.

3.5.2 Swimming morphology, kinematics and performance

It has previously been shown that higher swimming speeds in salps are related to higher pulse frequencies (Madin 1990). In the present study, the fastest-swimming species, *W. cylindrica*, also had the shortest jet periods, most streamlined form, lowest drag and the highest jet speeds (Tables 3.1, 3.2). Conversely, the slowest swimming species examined in this study, *P. confoederata*, produced the highest weight-specific thrust and swam with the greatest propulsive efficiency (Tables 3.1, 3.2). Swimming performance variables indicated that *C. affinis* was the weakest swimmer, exhibiting the lowest weight-specific thrust, highest drag and lowest whole-cycle propulsive efficiency (Table 3.2). However, the variables measured in this study relate to hydrodynamic efficiency which does not consider energetic cost of swimming. Across all species, both whole-cycle and rocket motor propulsive efficiency increased with speed with a

concomitant decrease in slip (Fig. 3.11b, c, d). A maximum efficiency and low slip at higher speeds might be beneficial for vertically migrating salp species, which travel hundreds of meters over a 24 hour cycle (e.g. Madin et al. 2006).

Swimming thrust and efficiency measurements from the current study differed from those measured in *Salpa fusiformis* (Bone and Trueman 1983). Thrust measurements in the two studies deviated by an order of magnitude and since *S. fusiformis* is similar in size, streamlining and swimming speed to *W. cylindrica*, this was unexpected. Bone and Trueman (1983) approximated thrust two ways: using measurements of static thrust and chamber pressure, as well as using estimates of mass and maximum acceleration. Since my measurements were based on jet velocity and jet area, it is not possible to resolve this discrepancy. Propulsive efficiency of *S. fusiformis*, calculated from maximum jet and body velocities in Bone and Trueman (1983) were much lower than those measured in the present study, ranging from 17- 46% though the authors reported that they would expect higher efficiencies at cruising speeds.

From the standpoint of the salp, whole-cycle propulsive efficiency is of greatest relevance for ecological performance. The equation for whole-cycle propulsive efficiency derived by Anderson and Demont (2000) has a maximum theoretical efficiency of 58% and *P. confederata* came close to achieving this upper bound, with a mean efficiency of 55% (Table 3.2). Nonetheless, even the species with the lowest measured mean efficiency of 47% (*C. affinis*) was still relatively efficient. Though the swimming efficiencies of blastozooid chains were not measured in this study, Bone and Trueman (1983) found that a chain of actively swimming *S. fusiformis* swam at even higher efficiencies than individual blastozooids or oozoids. Salps in this study had higher whole-cycle propulsive efficiencies than squid. Efficiency for the squid *L. brevis* ranges from 29- 44% and efficiency for the squid *L. pealei* ranges from 34- 48% (Bartol et al. 2001, Anderson and Demont 2000). In comparison to squid, salps have siphons on opposite ends of the body so losses due to intake are smaller. Salps swim continuously using a high volume, low velocity jet, which also drives a feeding current. Squid on the other hand, don't need swim continuously and can also rely on fin motion to aid in

swimming. For squid, speed and maneuverability may be enhanced at the cost of propulsive efficiency.

Though Froude efficiency underestimates efficiency of jetting, it provides a measure of hydrodynamic efficiency during jetting that can be compared with other aquatic swimmers. In terms of Froude efficiency, *P. confoederata* also out-performs the other species in this study with a mean efficiency of 67% (Table 3.2). Salps in general jetted at higher Froude efficiencies than the scallop, *Placopecten magellanicus*, which swam with a Froude efficiency of 50% (Cheng and Demont 1996). This is not surprising considering that scallops only swim in rare instances as an escape response. Though salps are capable of heroic propulsive efficiencies compared to other aquatic invertebrates, the highest Froude efficiencies are achieved by vertebrate swimmers. Rainbow trout, *Oncorhynchus mykiss*, swam at a mean Froude efficiency of 74 % (Nauen and Lauder 2002) while false killer whales, *Pseudorca crassidens*, swam at an impressive maximum Froude efficiency of 90% (Fish 1998).

3.5.3 Ecological and evolutionary context for swimming patterns

A comparison of swimming performance among this group of morphologically distinct organisms naturally leads to questions about the ecological function of swimming characteristics as well as evolutionary relationships. The production of isolated vortex rings, along with high weight-specific thrust and high whole-cycle propulsive efficiency of *P. confoederata* suggests that this species has evolved traits for highly economical swimming. Conversely, swimming by *C. affinis* is characterized by a trailing jet, low weight-specific thrust and whole-cycle propulsive efficiency. Intriguingly, a recent molecular phylogeny of the Thaliaceans supports *Pegea* spp. as part of an ancestral lineage, whereas the *Cyclosalpa* spp., occupies a more derived position, paraphyletic with the Salpinae (Govindarajan et al., in review). Since pumping fulfills a dual role of propulsion and feeding, one might surmise that though cyclosalps are poor swimmers, perhaps they are effective filter feeders. However, this is not the case. Though there is considerable scatter in filtration rate measurements depending on the methods used,

previous studies have generally shown *C. affinis* to have some of the lowest filtration rates (Madin and Deibel 1998). The most recent work, conducted in conjunction with this study, showed that *C. affinis* had the lowest normalized filtration rates, *P. confoderta* had intermediate rates and *W. cylindrica* had the highest rates, though with the exception of *W. cylindrica* aggregates rates were not significantly different between species (Chapter 2). It is also of interest that *W. cylindrica* is both fast-swimming and has high filtration rates. Both of these traits are likely tied to the high pulsation rates in this species.

Still, a complete picture of trade-offs in swimming and feeding requires consideration of energetic requirements of different species. Weight-specific respiration rates by *C. affinis* and other *Cyclosalpa* sp. are indeed low compared to other species, suggesting a lower energetic cost of locomotion (Madin and Deibel 1998). Faster swimming and more streamlined species, including *W. cylindrica* and *Salpa* spp., have some of the highest weight-specific respiration rates (Madin and Deibel 1998). Considering that several *Salpa* species make extensive diel vertical migrations, high swimming speeds that are also relatively hydrodynamically and energetically inefficient may be a necessary cost that is compensated by higher filtration rates. In conjunction with recent phylogenetic and filtration rate studies, the results of this work enhance our understanding of the evolution of diverse form and function in this important holoplanktonic group.

Chapter 4

Filtration of submicrometer particles by pelagic tunicates

4.1 Abstract

Salps are common in oceanic waters and have higher individual filtration rates than any other planktonic filter feeder. Though salps are centimeters in length, feeding via particle capture occurs on a fine mucous mesh (width = $1.4 \pm 0.5 \mu\text{m}$) at low velocities (1.6 cm s^{-1}) and is a low Reynolds number ($\text{Re} = 1.5 \times 10^{-3}$) and low Stokes number ($\text{St} \sim 8.5 \times 10^{-7} - 8.5 \times 10^{-1}$) process. Utilizing equations to model capture rate using a rectangular mesh and realistic oceanic particle concentrations, I show that compared to larger particles, submicron particles are encountered at the higher rates by the salp feeding apparatus. Results from feeding experiments with 0.5, 1 and 3 μm polystyrene microspheres corroborate model predictions. Though 1 to 10 μm -sized particles (e.g. flagellates, small diatoms) are predicted to provide four times as much carbon as 0.1 to 1 μm - sized particles (e.g. bacteria, *Prochlorococcus*), I estimate that particles smaller than the mesh size (1.4 μm) can fully satisfy salp energetic needs. Furthermore, salp swarms can substantially impact the particle size spectra in the ocean by removing different sized particles with nonuniform efficiency.

4.2 Introduction

Filter feeding as a mechanism of concentrating small food particles is common among marine plankton. Among marine filter-feeders, pelagic tunicates in the class Thaliacea, order Salpida, have the highest individual filtering rates (Alldredge and Madin 1982), with weight-specific clearance rates ranging from 70 and 4153 ml mg⁻¹ hr⁻¹ (Madin and Deibel 1998 and references therein). Particles are captured on a mucous filtering net with mesh widths on the order of 1 µm (Bone et al. 2003) and subsequently packaged into dense, mucus-bound fecal pellets that remain intact for days (Caron et al. 1989) and have sinking velocities ranging between 200 and 3646 m day⁻¹ (Madin et al. 2006, Phillips et al. 2009, Yoon et al. 1996), faster than most copepod or krill feces (Bruland and Silver 1981). Because of high filtering rates, small mesh size and rapidly sinking fecal pellets, salps have the potential to remove substantial amounts of primary production from surface waters and deliver it to the ocean's interior (Andersen 1998) where it can be an important contribution to export flux (Wiebe et al. 1979, Fortier et al. 1994). High individual growth rates and the alternation of life cycle stages between a solitary, asexual phase and an aggregate, sexual phase allow for rapid population growth when environmental parameters are optimal. Large salp aggregations could exert a particularly important influence on biogeochemical cycling and the structuring of planktonic communities (e.g. Madin et al. 2006).

Filtration by salps is accomplished by rhythmically pumping water into the oral aperture, through the pharyngeal and atrial chambers and out the atrial siphon. This pumping process also creates a propulsive jet for locomotion. Food particles entering the pharyngeal chamber are strained through a mucous net that is continuously secreted and rolled into a food strand that moves posteriorly towards the esophagus. The net, which is secreted by the endostyle, fills much of the pharyngeal cavity and resembles a bag-like plankton net (Fig. 4.1). The nature of the feeding mechanism is non-selective; any particles that enter the oral siphon and adhere to the filtering mesh will be ingested.

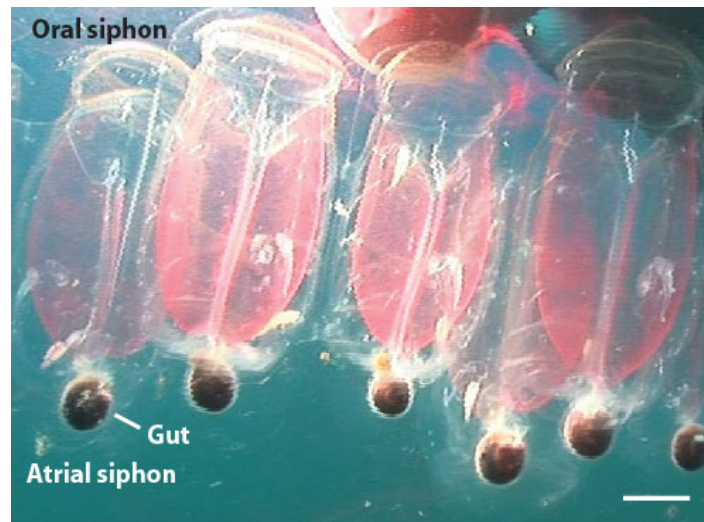


Fig. 4.1. *Pegea confoederata* aggregates. Mucous feeding filter made visible with carmine particles. Scale bar is 1 cm.

Though the basic mechanism of salp filter-feeding has been established (Madin 1974), an understanding of filtration efficiency and particle selectivity of tunicates requires investigation of the fluid mechanics at the level of the filtering mesh. Based on filter element diameter (~ 100 nm, Bone et al. 2003), filter mesh spacing (~ 1 μ m, Bone et al. 2003) and velocity at the mesh (0.6 cm s $^{-1}$, Madin 1990), fluid interactions at the mesh are characterized by a low-Reynolds-number regime. To understand how these biological filters perform, we must consider how particles interact with the mesh at the micron-scale.

Insight into the function of biological filters has advanced with the application of engineering principles to filtration mechanics (Rubenstein and Koehl 1977, Shimeta and Jumars 1991). Both theoretical models and experiments have confirmed that for marine filter feeders with rectangular meshes, mechanisms other than simple sieving allow for collection of particles that are smaller than the spacing between filtering elements. For example, models of filter efficiency by caddisfly larvae in stream beds (Silvester 1983, Loudon and Alstad 1990) and retention efficiency experiments with marine appendicularians using submicron particles (Deibel and Lee 1992, Fernández et al. 2004, Flood 1992) have demonstrated capture of particles much smaller than the mesh

dimensions via diffusional deposition and direct interception of particles on filter elements.

Mathematical models of the salp filtration process have been inapplicable due to a lack of accurate feeding parameters and empirical studies of size retention efficiencies have been limited by the particle sizes offered in the experiment or the sensitivity of the particle measuring method. Empirical feeding studies using naturally occurring particles, cultured cells and polystyrene beads have concluded that the salp size retention cut-off is 1-2 μm , but a limitation of these studies is that particles $< 1\mu\text{m}$ were below the detection limit of the measurement device (i.e. Coulter Counter, Harbison and Gilmer 1979) or were not introduced in feeding experiments (Caron et al. 1989, Kremer and Madin 1992). Though retention efficiency of particles $< 1\mu\text{m}$ remains inconclusive, *Synnechococcus* and other small cyanobacteria (0.7 -1 μm) have been removed by salps during feeding studies (Harbison and Gilmer 1979) and identified in salp fecal pellets (Caron et al. 1989, Silver and Bruland 1981). Images of salp filtering meshes acquired using scanning electron microscopy (SEM) and transmission electron microscopy (TEM) have provided measurements of the spacing and thickness of the filter strands and have also offered insight into the arrangement of mesh fibers (summarized in Bone et al. 2003). A limitation of the measurements, however, is that shrinkage of mucous meshes during preparation and processing made the spacing difficult to estimate, so the true mesh dimensions are unknown.

The focus of the present study is to understand whether low Re particle capture mechanisms are important for salp filtration, allowing for capture of particles smaller than the mesh dimensions. I made accurate measurements of filtration parameters, including mesh spacing and incurrent velocities, and applied them to a low Re number particle encounter model for rectangular meshes (Silvester 1983). Theoretical predictions were then compared to retention rates of 0.5, 1 and 3 μm fluorescent polystyrene microspheres by the salp species *P. confederata*. Using this combination of modeled predictions and feeding experiments I show that 1) salps can fulfill their energetic requirements with particles smaller than the mesh width and 2) salp aggregations can

have a substantial influence on carbon flow within the smallest size classes of particles in the ocean.

4.3 Methods

4.3.1 Collection of specimens

P. confoederata were collected in individual 800 mL plastic jars using bluewater SCUBA techniques (Haddock and Heine 2005) at the Liquid Jungle Lab off the Pacific coast of Panama (7° 50' N, 81° 35' W) during January 2007, 2008 and 2009. Animals were maintained in collection jars or in tanks of field-collected seawater at ambient temperature (26-28° C). All measurements were taken within 12 hrs of collection.

4.3.2 Parameter measurements

Filter mesh measurements of *P. confoederata* were obtained by viewing fluorescently-stained 'wet' filters under a fluorescence microscope. In order to remove part of the mesh, a section of a glass coverslip (~1 x 1mm) held by forceps was gently inserted through the oral siphon and swept through the pharyngeal chamber. If a piece of mesh was visible on the coverslip, it was placed on a microscope slide with a drop of fluorescent stain, fluorescein isothiocyanate-conjugated concanavalin A (FITC-ConA) from *Canavalia ensiformis* (SIGMA), in seawater solution. Images of the mesh were acquired using a Zeiss Axiostar Plus microscope with HBO 50 epifluorescence lamp and a Nikon Coolpix 8800 camera. The structure of the mesh only became visible when viewed at 1000x (10x ocular with 100x/1.45 n.a. oil immersion objective). This is the first time tunicate feeding filters have been imaged 'wet' using light microscopy and without chemical fixation; therefore meshes were not subject to shrinkage during preparation. Measurements were taken from six *P. confoederata* solitaires and three individual aggregates from 16 to 60 mm body length. Mesh length and width were measured in Image J (NIH) and a mean length and width for each individual was calculated based on multiple measurements.

Feeding current velocity and the flow pattern were determined using particle tracking or particle streak velocimetry. Individual *P. confoederata* were placed in custom-built acrylic tanks with field-collected seawater seeded with 8-12 μm titanium dioxide particles. Particles were illuminated from one side by a 30 mW, 500 nm laser directed through a cylindrical optic to form a 1-mm-thick light-sheet. Particle motions were videotaped with a Sony HDR-HC7 high definition camcorder (1440x1080 pixels, 30 fps). Velocities were determined by tracking individual particles between frames relative to reference frame landmarks on the salp body or by measuring particle streak lengths in a single frame using ImageJ (<http://rsb.info.nih.gov/ij>). Because salps are transparent, it was possible to track particles within the pharyngeal chamber just before contact with the filtering mesh.

4.3.3 Low Re particle capture model

The models of particle capture applied are appropriate for low Reynolds number ($\text{Re} = d_c u / \mu \ll 1$ where d_c is collector diameter, u is speed through the filter, ρ is fluid density and μ is dynamic viscosity) and low Stokes number ($\text{St} = d_p^2 u \rho / 18 \mu d_c \ll 1$ where d_p is particle diameter) (Silvester 1983). Parameters in the model were either direct measurements from this study (mesh dimensions, velocity through the filter), measurements from the literature (mesh fiber diameter, particle concentrations) or, seawater properties (seawater temperature, density and viscosity at 20° C). The primary mechanisms of particle capture for a filter feeder with a rectangular mesh are direct interception and diffusional deposition (Silvester 1983). Both models assume spherical particles and 100% adhesion to the mesh. Efficiency of direct interception for a single fiber is:

$$E_R = [2E_I \ln E_I - E_I + \frac{1}{E_I}] / \Lambda \quad (4.1)$$

where

$$E_I = 1 + \frac{d_p}{d_c} \quad (4.2)$$

$$\Lambda = 1 - 2 \ln \tau + \frac{\tau^2}{6} - \frac{\tau^4}{144} + \frac{\tau^6}{1080} \quad (4.3)$$

$$\tau = \frac{\pi d_f (h_1^2 + h_2^2)^{\frac{1}{2}}}{h_1 h_2} \quad (4.4)$$

h_1 is mesh width and h_2 is mesh length. Direct interception efficiency reaches 100% when particle size is equal to the mesh width. Direct interception models assume that particle diameter is much less than collector diameter and that mesh spacing is much greater than collector diameter, however, the expression is still realistic for larger particles that are small relative to the mesh opening (Silvester 1983). Efficiency of diffusional deposition for a single fiber is:

$$E_D = 2.9 \left(\frac{\Lambda}{2} \right)^{\frac{1}{3}} Pe^{-\frac{2}{3}} + 0.62 Pe^{-1}, \quad (4.5)$$

where Pe is the Péclet number

$$Pe = \frac{d_f u}{D} \quad (4.6)$$

and D is the Diffusivity of a non-motile particle

$$D = \frac{kT}{3\pi\mu d_p} \quad (4.7)$$

k is Boltzmann's constant ($1.38 \times 10^{-23} \text{ m}^2 \text{ kg s}^{-2} \text{ K}^{-1}$) and T is temperature (K).

Diffusivities of swimming particles were based on empirical measurements (Visser and Kiørboe 2006). The total fiber efficiency, E , is the sum of direct interception and diffusional deposition:

$$E = E_R + E_D \quad (4.8)$$

and the efficiency of a rectangular filter is

$$E_r = \frac{Ed_f}{h_e} \left[1 - \frac{Ed_f h_e}{h_1 h_2} \right] \quad (4.9)$$

where h_e is equivalent mesh spacing:

$$h_e = \frac{h_1 h_2}{(h_1 + h_2)} \quad (4.10)$$

The total encounter rate (particles s^{-1}), which directly relates to salp feeding ecology, is the product of capture efficiency, E_r (%), volume flow rate, Q ($ml\ s^{-1}$), and particle concentration (particles ml^{-1}):

$$P = E_r Q C \quad (4.11)$$

Volume flow rate ($Q = 1.69\ ml\ s^{-1}$) was an average determined for a 40 mm *P. confederata* from several studies (Chapter 2, Harbison and Gilmer 1976, Madin and Kremer 1995).

An evaluation of the literature yielded realistic concentrations for a range of particle diameters based on reviews or results from large scale oceanographic studies (Fig. 4.2). However, a regression equation relating cell diameter to cell concentration based on four Atlantic Ocean transects was used in the model (Cermeño and Figueiras 2008). Particle concentrations from the equation were lower than those from the literature review and were therefore more conservative estimates (Fig. 4.2). Volume and carbon encountered were calculated by converting diameter to volume ($V = (\pi d_p^3)/6$) and using a volume to carbon conversion for phytoplankton ($C = 0.11 V^{0.99}$; Montagnes et al. 1994). Because undigested particles as small as $1\ \mu m$ are frequently observed in salp fecal pellets (e.g. Caron et al. 1989, Silver and Bruland 1981), I also explored the implications for carbon encounter if only the outer $0.1\ \mu m$ of each particle is digested. To put model results in the context of salp feeding ecology, carbon encounter rate was compared to salp carbon ingestion and I estimated the impact of salp grazing on particle size spectra in the ocean.

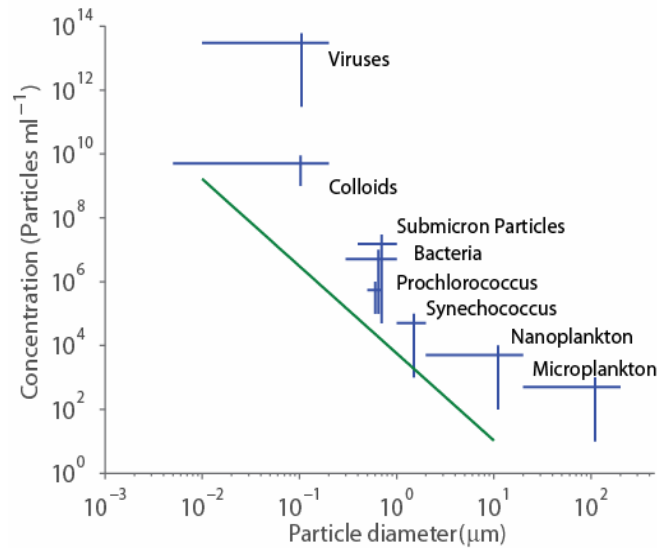


Fig. 2. Size range and abundance of various living and non-living particles in the upper ocean including viruses (Fuhrman 2000), colloids (Wells and Goldberg 1994), submicron particles (Yamasaki et al. 1998), bacteria (Caron et al. 1995; Li 1998), *Prochlorococcus* (Partensky et al. 1999), *Synechococcus* (Li 1998), nanoplankton (Caron et al. 1995; Dennett et al. 1999), and microplankton (Caron et al. 1995; Dennett et al. 1999). Line is regression of microphytoplankton concentration versus size from four Atlantic Ocean transects (Cermeño and Figueiras 2008) with cell volume converted to cell diameter.

4.3.4 Particle capture experiments

Relative retention efficiencies of 0.5, 1 and 3 μm fluorescent polystyrene microspheres (Polysciences, Inc.) were determined during two feeding experiments. Microspheres were treated with 5 mg ml⁻¹ bovine serum albumin for 12-48 hours to avoid clumping (Pace and Bailiff 1987). As salps behave most normally when disturbance is minimized, experiments were conducted in collection jars within 3 hrs of collection. At the start of the first experiment, microspheres were added to each jar to achieve a concentration of approximately 10³ microspheres ml⁻¹ for each size. After two hours, *P. confederata* guts were excised and ground along with several microliters of seawater using a mortar and pestle. Two 2 μl subsamples of the homogenate were examined using epifluorescence microscopy and particles of each size were counted from three fields from each 2 μl subsample. It was possible to distinguish the three particle sizes because they emitted at different wavelengths (0.5, 1 and 3 μm particle emission maxima were 486,

407 and 486 nm respectively). By counting a total of six fields, there were a minimum of 50 particles for the most abundant size-class. A second experiment was conducted to more accurately represent the higher concentrations of small particles in the marine environment. The protocol was identical, but the starting concentrations of 0.5, 1 and 3 μm particles were 10^5 , 10^4 and 10^3 particles ml^{-1} , respectively. For both experiments, relative retention efficiencies were determined by dividing the count for a given particle size by the total count of all three particle sizes. Experimental results were then compared to predictions based on calculations of low Re number filtration and simple sieving.

4.4 Results

4.4.1 Mesh dimensions and particle speeds

Images of the mucous filtering mesh revealed a regularly spaced rectangular mesh with thicker transverse strands. In some cases, it appeared that there were additional strands in a different plane and these strands tended to be at oblique angles to the primary rectangular mesh or appeared to be tangled (Fig. 4.3). The mean mesh width and length dimensions were $1.4 \pm 0.5 \mu\text{m}$ and $6.0 \pm 1.5 \mu\text{m}$ respectively ($n=9$) and mesh width increased with body length (Fig. 4.4).

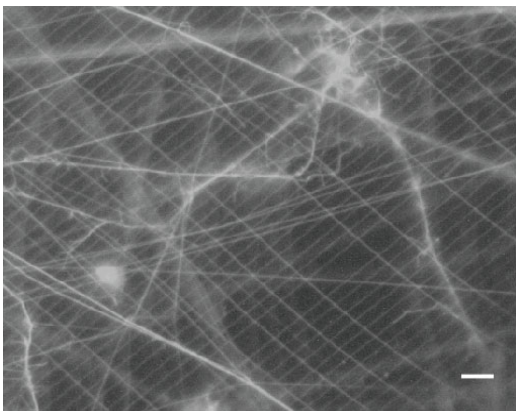


Fig. 4.3. Microscope image of fluorescently stained *P. confoederata* mucous filtering mesh. Scale bar is 5 μm .

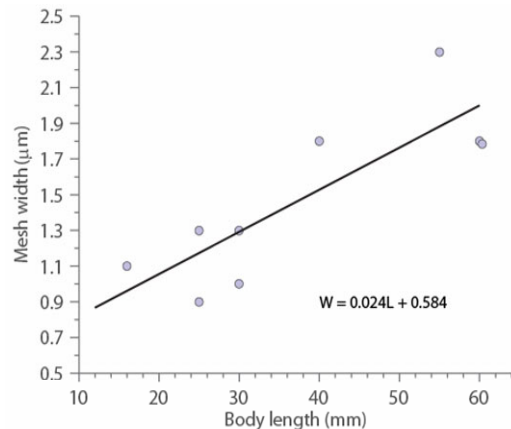


Fig. 4.4. Mesh width (W) as a function of *P. confoederata* body length (L). Linear regression equation shown in green ($W = 0.024L + 0.584$; $n = 9$; $r^2 = 0.70$).

Flow visualization using particle streaks provided both accurate fluid speeds near the filter and a qualitative picture of feeding currents. The mean velocity and maximum velocity were 1.63 and 3.81 cm s^{-1} , respectively (Table 4.1). Particle trajectories showed that fluid is drawn in around the edges of the oral siphon as it opens such that the area directly in front of the siphon is relatively undisturbed. As fluid enters the pharyngeal cavity it accelerates and then moves in a circular pattern suggesting that particles impact the filter tangentially.

Table 4.1. *P. confoederata* incurrent particle speeds. Speed and standard deviation (SD) for each individual are based on multiple measurements (n).

Individual	Stage	Body length		Mean speed (cm s^{-1})	Max speed (cm s^{-1})
			(mm)		
1	Agg		27	2.30 ± 1.12 (3)	4.11
2	Sol		30	1.22 ± 0.86 (9)	4.10
3	Sol		34	1.53 ± 0.52 (15)	2.40
4	Sol		53	1.89 ± 1.02 (13)	3.93
5	Sol		56	2.04 ± 1.82 (11)	6.66
6	Sol		62	0.81 ± 0.23 (14)	1.63
				Mean \pm SD (n)	Mean \pm SD (n)
				1.63 ± 0.55 (6)	3.81 ± 1.74 (6)

4.4.2 Model predictions

Filtration at the level of the *P. confoederata* filtering mesh is a low Reynolds number ($\text{Re} = 1.5 \times 10^{-3}$ where $d_c \sim 100 \text{ nm}$, Bone et al. 2003) and low Stokes number process ($\text{St} \sim 8.5 \times 10^{-7} - 8.5 \times 10^{-1}$ for d_p , particle diameter, ranging between 10^{-8} to 10^{-5} m). The model showed that both diffusional deposition and direct interception play a role in particle encounter for salp filtering meshes (Fig. 4.5). For particles ranging in size from about 0.01 to $0.05 \text{ }\mu\text{m}$ in diameter (viruses, colloids, bacteria), diffusion is the primary mechanism of particle encounter, though efficiency is less than 2%. For particles larger than $0.3 \text{ }\mu\text{m}$, swimming particles have higher diffusional encounter compared to non-motile particles. Below $0.3 \text{ }\mu\text{m}$, swimming is unlikely as Brownian rotation turns the bacterium too frequently for swimming to be effective (Dusenbery 2009). All particles

above about 0.05 μm are orders of magnitude more efficiently captured via direct interception compared to diffusional deposition.

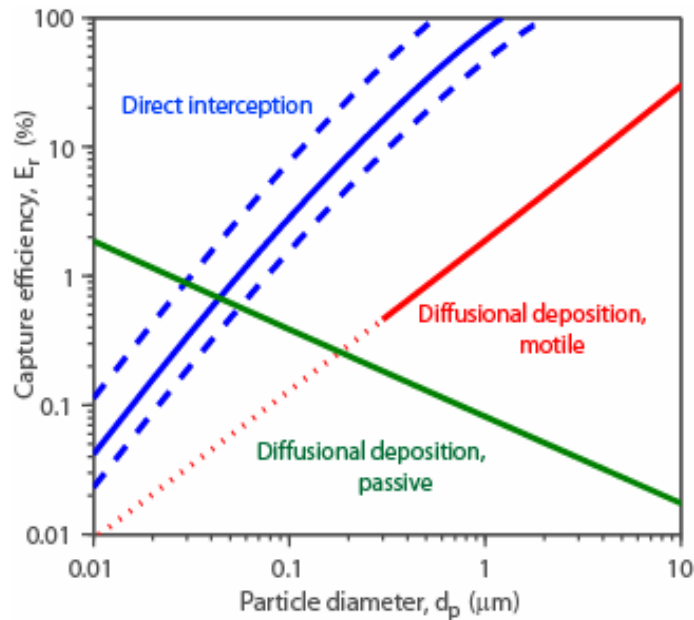


Fig. 4.5. Particle capture efficiency predicted for *P. confoederata* over a range of particle sizes. Efficiency of direct interception (blue) shown with lower and upper bounds (dashed lines) based on minimum and maximum measured mesh width (0.5 - 2.3 μm ; Table 4.1). Efficiency of diffusional deposition of passive particles shown in green and of motile particles shown in red (motility parameters from Visser and Kjørboe 2006) Dashed section of red line indicates that below 0.3 μm motility is not possible (Dusenbery 2009).

Because there are substantially higher numbers of small particles in the ocean (Fig. 4.2), these particles can be disproportionately ingested even when encounter efficiencies are relatively low. Estimates of particle encounter based on encounter efficiency, volume flow and realistic particle concentrations (Eq. 4.1) show that particles in the 0.01 to 0.1 μm range (viruses, colloids) are captured at 195 times the rate of particles in the 0.1 to 1 μm size range (submicron particles, bacteria, *Prochlorococcus*) (Fig. 4.6a). Though smaller particles are encountered at much higher rates, larger particles still contribute more volume and carbon. Particles in the 0.1 to 1 μm size range contribute 38 times more carbon than 0.01 to 0.1 μm particles. However, particles in the 1 to 10 μm size range contribute just four times as much carbon as those in the 0.1 to 1

μm size range (Fig. 4.6b). Assuming that only the outer 0.1 μm of each particle is digested, most of the carbon contribution would come from particles on the 0.1 to 1 μm size range with the maximum carbon from 1.1 μm - diameter particles (Fig. 4.6b).

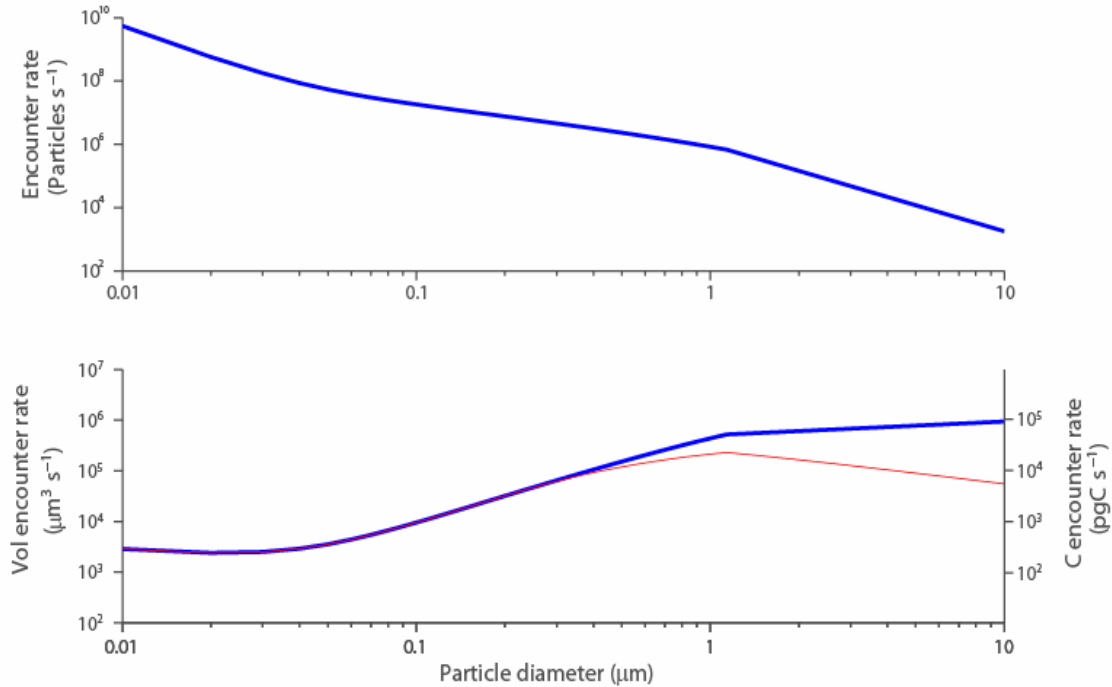


Fig. 4.6. Combined encounter rate predicted for diffusional deposition and direct interception as a function of particle diameter for *P. confoederata*. Particle concentrations based on relationship between microphytoplankton size and concentration (Cermeno and Figueiras 2008, Fig. 4.4). Volume flow rate = 1.69 ml s^{-1} (average from Harbison and Gilmer 1976, Madin and Kremer 1995, Chapter 2). (A) Particle encounter rate (B) Volume and carbon encounter rates (blue line) and volume and carbon encounter rate assuming an outer shell of 0.1 μm can be digested (red). Cell volume (μm^3), V , to carbon (pg cell^{-1}), C , conversion for phytoplankton is $C = 0.11V^{0.99}$ (Montagnes et al. 1994).

In spite of the substantial carbon contribution from larger particles, the model shows that particles $< 1.4 \mu\text{m}$ (1.4 μm is mean mesh width) supply a total of $0.15 \text{ mg C hr}^{-1}$. The carbon ingestion rate of a 40 mm *P. confoederata* aggregate is $2.2 \% \text{ body C hr}^{-1}$ (Cetta et al. 1986) which equates to a requirement $0.02 \text{ mg C hr}^{-1}$ based on a carbon to live length relationship (Madin et al. 1981). Therefore, the carbon supplied by particles

smaller than the mesh opening has the potential to supply more than 7 times the energetic requirement.

4.4.3 Feeding experiments

Experimental results tested how accurately the model predicted encounter efficiency. When the same concentration of each particle size was offered, capture rate was similar among sizes with a slight preference for the larger particles (Fig. 4.7a). Mean relative capture rates (\pm SD) of 0.5, 1 and 3 μm particles were $29.1 \pm 8.6\%$, $30.1 \pm 5.4\%$ and $40.8 \pm 12.9\%$, respectively. Modeled filtration based on direct interception (relevant for particles $> 0.1 \mu\text{m}$) was comparable to experimental capture efficiency with relative capture rates for 0.5, 1 and 3 μm particles of 13.8 %, 32.9 % and 53.3 %, respectively. Simple sieving was an inferior predictor of relative capture rate and was particularly poor at predicting capture rates of the smallest particles. Relative capture rates predicted for simple sieving of 0.5, 1 and 3 μm particles were 3.7 %, 14.5 % and 81.9 %, respectively. Offering different concentrations of particles provided a more realistic simulation of the particle assemblage available in the ocean and as in the first experiment, the experimental results were most similar to the direct interception model, and not the simple sieving model (Fig. 4.7b). Notably, a higher proportion of the 0.5 μm particles were captured in both experiments than either model predicts.

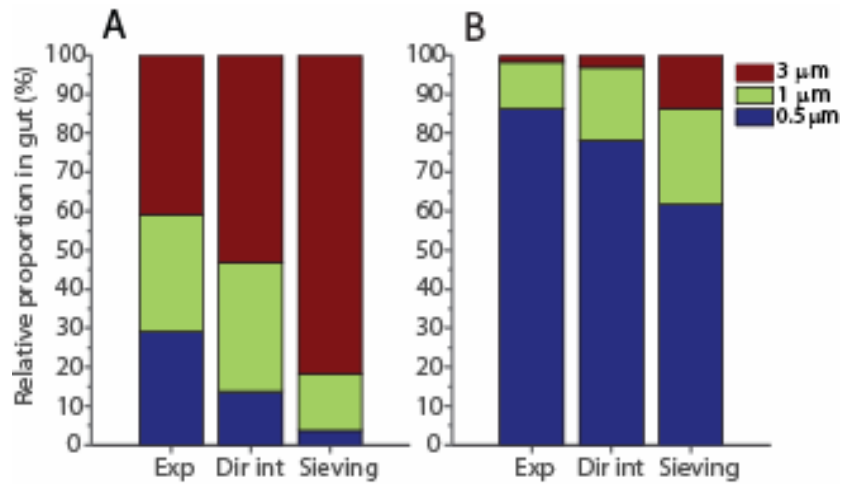


Fig. 4.7. Relative proportions of 0.5, 1 and 3 μm microspheres in *P. confoederata* gut after feeding experiments (Exp) compared to relative proportions predicted by direct interception (Dir int) and simple sieving (Sieving). (A) Equal initial concentrations of each particle size class (10^3 particles ml^{-1}). (B) Initial concentrations particles varied to more accurately reflect marine particle size spectra (0.5, 1 and 3 μm particle concentrations were: $\sim 10^5$, $\sim 10^4$ and $\sim 10^3$ particles ml^{-1} , respectively).

4.5 Discussion

A combination of mathematical predictions and experiments in the context of oceanic particle size spectra show that simple sieving is not the dominant feeding mechanism for salps and, at least for *P. confoederata*, the energetic requirements of salps can be completely met by particles that are smaller than the filtering mesh dimensions. Filter feeding by salps is a low Reynolds number and low Stokes number process that occurs via diffusional deposition and direct interception. Due to high filtration rates, salps are capable of removing substantial energy from the smallest particles in the ocean, which is transferred to higher trophic levels or exported to deeper water via the sinking of large fecal pellets or salp carcasses. This filtration capacity becomes magnified when salps periodically form blooms.

4.5.1 Model parameters

A model is only of value if the parameters are realistic. One of the strengths of the model results was the use of appropriate parameter values based on direct measurements in laboratory studies. Images of the mucous filtering mesh from this study represent the first obtained using unfixed ‘wet’ meshes. The resultant mean mesh width was at least two times higher than previous *Pegea* sp. measurements from TEM or SEM images, where drying and shrinking occurred (Bone et al. 1991, Silver and Bruland 1981). Nonetheless, even wet meshes may have been stretched or distorted during removal and the optimal situation would be to image the mesh *in situ*. The finding that mesh spacing increases with body size (Fig. 4.4) supports previous conclusions that smaller salps retain smaller particles (Harbison and McAlister 1979, Kremer and Madin 1992). As suggested by Bone (2003), mesh size is likely dictated by ciliary spacing within the endostyle, which also increases with body size. The elongate rectangular mesh shape, instead of a square mesh, is also present in other aquatic filter-feeders including appendicularians and caddisfly larvae and may serve to optimize particle capture while minimizing the amount of material required (Wallace and Malas 1976).

Flow visualization using particle streaks provided accurate velocities at the capture surface and also provided an improved understanding of the feeding mechanism. With a mean of 1.63 cm s^{-1} , *P. confederata* feeding current speeds (Table 4.1) are much higher than appendicularians (*Oikopleura vonhoffeni*: $0.056\text{--}0.32 \text{ cm s}^{-1}$; Acuña et al. 1996, Morris and Deibel 1993) and doliolids (*Dolioletta gegenbauri*: 0.11 cm s^{-1} ; Bone et al. 1997), which also use mucous filters but create a current by ciliary beating instead of muscular contractions. Feeding-current speeds of salps are closer to those of crustaceans, which are generated by coordinated movements of feeding appendages. The copepod *Temora longicornus* generates a mean feeding current of 0.63 cm s^{-1} (van Duren et al. 2003) and the krill *Euphausia pacifica* generates a current that is less than 1 cm s^{-1} in the region of the thoracic legs (Yen et al. 2003). Though salp and crustaceans filter at similar speeds, salps process much higher fluid volumes than their crustacean counterparts.

Qualitative visualization of the flow field pattern shows that the filtering system is likely effective at capturing both motile and nonmotile particles using tangential flow filtration (TFF). The relatively quiescent flow in front of the oral siphon is likely advantageous for capturing motile particles that would otherwise escape in response to a fluid mechanical disturbance. Once particles enter the pharyngeal chamber, circular fluid motion may result in particle trajectories that are parallel to the filtering mesh and concentration of particles via TFF. TFF is a technique used for concentrating particles from a large volume of solution and is particularly useful if the particles of interest are dilute in the solution. This technique has been used by aquatic scientists to concentrate colloidal material (Buessler et al. 1996, Whitehouse et al. 1990). In TFF, particles larger than the mesh become concentrated on the inside of the filter membrane through repeated cycling through the system and the membrane is less prone to clogging. Similar to TFF, the circulation of particles within the filtering mesh of *P. confederata* might serve to concentrate the particles without clogging the filtering apparatus, and the particles are subsequently collected on the mesh.

4.5.2 Limitations of model

Assumptions and simplifications made in the particle capture model limit its application. The equations for diffusional deposition and direct interception on a rectangular mesh assume spherical particles and 100% adhesion to the mesh. Adhesive properties of the mucous as well as surface chemistry of the particles are important for capture. For example, Gerritson and Porter (1982) found that *Daphnia magna* retained particles with a negative surface charge at lower efficiencies than those with a neutral surface and retained particles with a hydrophobic surface at lower efficiencies than those with a hydrophilic surface. In this study, the treatment of particles with BSA, which is negatively charged and hydrophilic, may have influenced capture rates. A greater understanding of the chemical properties of the mucous filter will be needed to interpret the role of surface chemistry in particle capture. Nonetheless, in this study experimental

capture rates of the smallest particles (0.5 μm) were actually higher than the model predicted, indicating that the model predictions were conservative.

4.5.3 Importance of submicron particles for salps

Considering that 1-2 μm has been deemed the filtration size cutoff for salps (Bone et al. 2003, Madin and Deibel 1998), our finding that submicron particles are encountered frequently recasts our understanding of salp dietary composition. Particles in the 0.01 to 1 μm range (colloids, viruses) are captured primarily via diffusional deposition at very low efficiencies (Fig. 4.5) but because of the high concentrations of small particles in many marine environments (Fig. 4.2), these particles are encountered at the highest rates (Fig. 4.6a). Particles greater than 0.1 μm are primarily encountered via direct interception with efficiencies tending towards 100% as the mesh width is approached (Fig. 4.5). Though particles above 0.1 μm are encountered with greater efficiency, fewer larger particles would be encountered in most marine environments, because larger particles are present at lower concentrations (Fig. 4.2). Experiments with *P. confoederata* verify model predictions, actually showing higher encounter with the smaller particles than anticipated (Fig. 4.7). However, the majority of carbon is supplied by particles in the 0.1 to 1 μm (bacteria, *Prochlorococcus*) and 1-10 μm ranges (flagellates, small diatoms) (Fig. 4.6b). Volume increases proportionally to particle diameter cubed so larger particles contain disproportionately more carbon. In other words, it takes many small particles to provide the same amount of nutrition as one larger particle. On the other hand, if salps are unable to completely digest larger particles as evidenced by fecal pellet contents, larger particles may be less nutritionally valuable (Fig. 4.6b). Further study will be needed to determine digestion rates of various particle types especially considering that morphological and chemical properties of particle coating (cell walls, exoskeletons, plates, spines) may be as important as particle size. The prospect that submicron particles can fulfill the energetic requirements of *P. confoederata* helps to explain why the majority of salp species are found in oligotrophic waters, which are dominated by small plankton. Further mesh dimensions measurements of species

besides *P. confoederata* will be needed to confirm that other species fulfill energetic requirements with submicron particles. For example, *W. cylindrica* has higher energetic requirements than *P. confoederata* (Madin and Deibel 1998) but also has higher individual filtration rates which would result in higher encounter rates of all particle sizes (Chapter 2).

4.5.4 Impact of salps on marine ecosystems

Salp filtration rates are among the highest in marine environments, ranging from 0.01 to 15.33 ml s⁻¹ (Chapter 2, Madin and Deibel 1998). By constantly pumping large volumes of seawater through their bodies and retaining micron-scale particles, salps are well-adapted for existence in the oligotrophic ocean. Carbon in the pelagic environment is typically regenerated on the order of hours via the microbial loop. Salps and other pelagic tunicates remove particles that are around 4 orders of magnitude smaller than themselves, thereby bypassing several trophic levels (Fortier et al. 1994). Particles are packaged into membrane bound fecal pellets that are often incompletely digested and are therefore rich in carbon, nitrogen and phosphorous (Anderson 1998), and also contain trace elements (e.g. calcium, magnesium; Caron et al. 1989). Fecal pellets sink quickly and are transferred to a longer-lived pool in deeper water where material is sequestered on time scales of 1000 years or more. Thus, the presence of salps, particularly in bloom proportions, has the potential to profoundly influence biogeochemical cycling within microbial-dominated food webs. The efficiency with which salps repackage and export carbon from surface waters is underscored by a recent proposition to increase salp numbers globally in an effort to mitigate climate change (Kithil 2006). While the practicality of engineering salp populations blooms for this purpose has yet to be demonstrated, our results confirm earlier conclusions that salps are optimal grazers for the collection, repackaging and sedimentation of a wide range of particle sizes in the ocean (Alldredge and Madin 1982, Anderson 1998).

Chapter 5

Conclusions

5.1 Thesis summary

Salps are highly effective at pumping water through their bodies to drive a feeding current as well as a propulsive jet. Considering the diverse morphologies among salps and their wide, overlapping distributions, the central questions of this dissertation related to trade-offs between swimming and filtration between salp species and life-cycle stages. This study was conducted at the Liquid Jungle lab in Panama where salps were reliably available during the dry season (early January – early April) and the key species investigated were *Pegea confoederata*, *Weelia (Salpa) cylindrica* and *Cyclosalpa affinis*. The major findings of the dissertation were the following:

- 1) Filtration rates measured from *in situ* video kinematics yielded higher rates than previously reported, setting an upper limit on feeding capacity. Individual traits, including pulse rate and degree of compression, varied among species, but volume-normalized filtration rates were not significantly different among species with the

exception of *W. cylindrica* aggregates, which filtered with the highest rates. The implication is that salp species have converged on a flow optimum.

2) Flow visualization of the jet wake using *in situ* fluorescein dye and laboratory particle image velocimetry (PIV) showed that salps swim using vortex ring propulsion, but there are differences in the wake structure among species. Though *W. cylindrica* was the most streamlined and the fastest swimming species investigated, the slow-swimming *P. confoederata* produced the highest weight-specific thrust and highest whole-cycle propulsive efficiency. The slow-swimming *C. affinis* produced the highest drag, lowest weight-specific thrust and lowest whole-cycle propulsive efficiency. However, weak hydrodynamic performance may be compensated by relatively low energetic demands.

3) A low Reynolds number model of particle capture by salps showed that at realistic oceanic particle concentrations, submicron particles are captured at higher rates than larger particles. Though particles greater than 1 μm supply a greater proportion of carbon, particles smaller than the measured mesh size (1.4 μm) can satisfy a salp's energetic needs. Data from feeding experiments using 0.5, 1 and 3 μm polystyrene microspheres corroborated model results. By packaging submicrometer particles into rapidly sinking fecal pellets, salps can substantially change particle size spectra and contribute to vertical fluxes in the ocean.

5.2 Co-evolved swimming and feeding traits

Taken together, data from chapters 1 and 2 address the trade-offs between filtration and jet propulsion. These findings can be considered along with previous measurements of energetic parameters to understand the equilibrium of traits within each species. A summary of the filtration parameters from the first chapter and swimming performance parameters from the second chapter along with energetic parameters from the literature is presented in Table 5.1. The suite of traits present in each species can be

further considered in the context of phylogenetic relationships amongst the Thaliaceans (Govindarajan et al., in Review).

Table 5.1. Summary of filtration, swimming and energetic parameters of salps species investigated in this study. Data from solitary and aggregate generations are combined because relative values are comparable.

	<i>P. confoederata</i>	<i>W. cylindrica</i>	<i>Cyclosalpa spp.</i>
Swimming speed	Low ¹	High ¹	Int. ¹
Pulse rate	Int.	High	Low
Fineness	Low	High	Int.
FILTRATION			
Volume filtered	High	Low	Int.
Normalized vol. filtered	Int.	High	Low
SWIMMING			
Weight-specific thrust	High	Int.	Low
Drag	Int.	Low	High
Whole-cycle propulsive efficiency	High	Int.	Low
ENERGETICS			
Oxygen consumption	Int. ^{2,4}	High ^{2,4}	Low ^{2,3}
Carbon ingestion	Low ²	High ²	Int. ³

¹ Madin 1990, ² Cetta et al. 1986, ³ Madin and Purcell 1992, ⁴ Biggs 1977

5.2.1 *Pegea confoederata*

The slow-swimming *P. confoederata* has the least streamlined form and is thought to have the simplest chain architecture (Madin 1990). Individual-based filtration rates are high but normalized filtration rate is average. Unexpectedly, this species is the most economical swimmer of those investigated, with both highest thrust and highest whole-cycle propulsive efficiency. Moreover, compared to other species, oxygen requirements and carbon ingestion are relatively low (Biggs 1977, Cetta et al. 1986). In summary, considering that salps share the same food source, *P. confoederata* might be considered the ideal salp. Indeed, on the basis of morphology, this species has formerly been considered more derived (Metcalf 1918), which might seem consistent with results presented here. However, a recent phylogenetic analysis shows *P. confoederata* is one of

the more basal salp species, consistent with Madin's (1990) interpretation of chain architecture and swimming style (Govindarajan et al., in Review). There may be other ramifications of slow (albeit economical) swimming such as poor predator evasion or lowered reproductive encounter rates.

5.2.2 *Weelia cylindrica*

Similar to *Salpa* species, fast-swimming in *W. cylindrica* is accompanied by a streamlined solitary form and linear aggregates (Madin 1990). Though individual filtration rates are low in this species due to comparatively small body size, normalized filtration rates were significantly higher than any other species or lifecycle stage. Drag was low in *W. cylindrica* due to a fusiform morphology, but thrust and whole-cycle propulsive efficiency were average. Much like a sports car, *W. cylindrica* is fast but not necessarily efficient. High swimming speeds are achieved at the cost of high oxygen and carbon consumption rates. Though it has been recently established that *W. cylindrica* is not closely related to the *Salpa* species (Govindarajan et al, in Review), they share analogous chain architecture and high swimming speeds. Fast swimming may be advantageous for avoiding predation and also allows for vertical migration in some species from depths greater than 1000 m to the surface each day (Madin et al. 2006). This behavior may enhance reproductive exchange when aggregates are clustered in the surface waters.

5.2.3 *Cyclosalpa* species

The slow-swimming *Cyclosalpa* species have the lowest normalized filtration rates as well as the lowest hydrodynamic efficiency, suggesting this is a primitive group. Likewise, previous studies have suggested that the cyclosalps are relatively basal on the basis of morphology and chain architecture (Madin 1990, Metcalf 1918). However, a molecular phylogeny shows *Cyclosalpa* species to be more derived (Govindarajan et al, in Review). Notably, cyclosalps have comparatively low oxygen consumption and carbon ingestion rates and therefore, may be quite energetically efficient. There may be

other unknown aspects of *Cyclosalpa* biology relating to reproductive success or life-history strategy that enhance its ecological role.

Individual feeding and swimming traits aside, salp species collectively have the highest individual filtering rates of all filter feeders (Alldredge and Madin 1982). In chapter 3, I showed that salps have higher capture rates on submicron particles than previously thought and that particles below the mesh size can in fact fulfill the energetic requirements of *P. confederata*. This result warrants further study into the impact of salps on oceanic particle size spectra, particularly during salp blooms. Ideally, further work would involve live plankton and particulate organic material at realistic concentrations. Though I found a relationship between salp body length and mesh width, it remains to be seen whether different species of salps have different mesh dimensions. Small deviations in mesh size could dramatically influence the size range of food particles that are ingested. Contrary to the suggestion that salps are non-selective filter feeders, it is possible that different species ingest different size ranges of food items on the basis of mesh size.

5.2.4 Paradox of the plankton

The question of how biodiversity is maintained has a long history in community ecology and it is an interesting exercise to explore which hypothesis best explains the co-occurrence of salp species. Different swimming and feeding strategies among salp species hint at the concept of niche specialization. However, salps inhabit a seemingly homogenous environment and have wide and overlapping distributions and are also considered to share a similar diet. The question of how diverse morphologies with individualized function may have co-evolved in salps conjures a central theme in Biological Oceanography: Hutchinson's Paradox of the Plankton (Hutchinson 1961). Hutchinson questioned how a wide diversity of phytoplankton could be maintained in an unstructured ocean. Hutchinson touched on several possible mechanisms that might allow for stable coexistence of species, including temporal changes in environment,

predation, symbiosis and commensalism. All of these mechanisms could be important for salps though little is known about how these variables might impact species unequally. For example, all salps are relatively slow moving and would likely be captured at equal rates by a predator (Harbison 1998).

The notion of niche partitioning has been challenged more recently by Hubbell's neutral theory of biodiversity, which assumes that differences in species comprising an ecological community are unrelated to relative success (Bell 2001). Neutral community models consider that species are equivalent in terms of competitive ability, or fitness, and can still explain community diversity. Though it is tempting to assign this theory to salps and other oceanic filter feeders to explain the range in morphologies in spite of a homogeneous environment, there may be an interplay of very subtle environmental and ecological aspects that have maintained a diversity of salp species, as suggested by Hutchinson. Neutral theory and the more classic niche differentiation are endpoints on a continuum (Leibold and McPeck, 2006) and both mechanisms might help to explain the existence of an oceanic filter-feeding community.

5.3 Future applications

The work presented in this thesis naturally leads to a number of other questions, particularly in light of recent research trends. Below I will discuss a number of potential research directions that follow from this work.

5.3.1 Biogenic mixing

An ongoing debate about the importance of animals for ocean mixing has focused on the production of kinetic energy in the wakes of swimming animals (e.g. Dewar et al. 2006, Huntley and Zhou 2004). However, this research has been challenged by the suggestion that turbulence generated by most swimming animals in the sea occurs at small length scales and therefore dissipates rapidly as heat (Visser 2007). Most recently, a different mechanism of ocean mixing has been proposed; Darwinian induced fluid drift involves transport of viscous fluid that is carried along by swimming animals as they

move through a stratified ocean (Katija and Dabiri 2009). Measurements of jellyfish swimming in a stratified lake showed that mixing was dominated by this mechanism. Similarly, salps might have an important effect on ocean stirring, particularly on local scales when they occur in large, vertically migrating aggregations (e.g. Madin et al. 2006, Wiebe et al. 1979). According to Darwin's mechanism, a higher propulsive efficiency correlates to a higher contribution of induced drift relative to the kinetic energy lost in the wake (Katija and Dabiri 2009). Since salps have a comparatively high propulsive efficiency (Chapter 2) and low wake turbulence dissipation rates (Fuchs and Sutherland, unpublished data) compared to other plankton, salp swimming may be an important source of animal-induced mixing.

5.3.2 Coordinated swimming

One of the more fascinating aspects of salp swimming is the coordination of individuals in an aggregate chain. Though swimming is coordinated, pumping by zooids is asynchronous except during an escape response (Bone and Trueman 1983). Muscle contractions become simultaneous during escape, resulting in higher swimming speeds. Further, backwards swimming is sometime initiated as an escape response. Swimming efficiency of an entire aggregate was not measured in this thesis and the wake structure of multiple zooids in a chain was only marginally considered (Chapter 3). Yet, the swimming of chains is of key importance for the ecological roles of salp species. A deeper investigation of this problem will require three dimensional body kinematics and flow visualizations. The outcome of such studies could potentially be used in an applied sense. Though the evolutionary process is blind and therefore can not strive for optimality, a comparative approach reveals outcomes of different functional characteristics (Vogel 2003, pp. 508-517). Swimming efficiently may not be important for salp species that are merely pumping to drive a feeding current but by comparing species, it becomes evident which designs correlate with fast swimming and/or hydrodynamic efficiency. Further, the convergence of characteristics like streamlined

shape, linear chain geometry and fast swimming in both *W. cylindrica* and the Salpinae hints at functional significance of these properties.

5.3.3 Optimized filtration

The same argument, that nature does not strive for optimality, applies to filtration capacity. Yet, again, a comparative approach reveals which morphological and functional characteristics relate to a relatively higher filtration rate. Though differences in low Reynolds number filtration among species were not investigated in Chapter 4, it would be interesting to further investigate how the different combinations of volume flow-rate (Chapter 2) and small-scale particle capture might relate to filtration capacity.

References

- Acuña, J. L., D. Deibel, and Morris, C. C. (1996). Particle capture mechanism of the pelagic tunicate *Oikoplura vanhoeffeni*. *Limnol. Oceanogr.* 41: 1800-1814.
- Adrian, R. J. (1991). Particle imaging techniques for experimental fluid mechanics. *Ann. Rev. Fluid Mech.* 20, 421- 485.
- Alexander, R. M. (2003). Principles of animal locomotion. Princeton: Princeton University Press.
- Allredge, A. L. and Madin, L. P. (1982). Pelagic tunicates: unique herbivores in the marine plankton. *BioSci.* 32, 655-663.
- Andersen, V. (1985). Filtration and ingestion rates of *Salpa fusiformis* Cuvier (Tunicata: Thaliacea): Effects of size, individual weight and algal concentration. *J. Exp. Mar. Biol. Ecol.* 87: 14-29.
- Andersen, V. (1998). Salp and pyrosomid blooms and their importance in biogeochemical cycles. In: Bone Q (ed) *The biology of pelagic tunicates*. Oxford University Press, New York, pp 125-137.
- Anderson, E. J. and Demont, M. E. (2000). The mechanics of locomotion in the squid *Loligo pealei*: Locomotory function and unsteady hydrodynamics of the jet and intramantle pressure. *J. Exp. Biol.* 203, 2851-2863.
- Anderson, E. J. and Grosenbaugh, M. A. (2005). Jet flow in steadily swimming adult squid. *J. Exp. Biol.* 208, 1125-1146.
- Bartol, I. K., Krueger, P. S., Stewart, W. J., and Thompson, J. T. (2009). Hydrodynamics of pulsed jetting in juvenile and adult brief squid *Lolliguncula brevis*: evidence of multiple jet 'modes' and their implications for propulsive efficiency. *J. Exp. Biol.* 212 (12), 1889-1903.
- Bartol, I. K., Patterson M. R., and Mann, R. (2001). Swimming mechanics and behavior of the shallow-water brief squid *Lolliguncula brevis*. *J. Exp. Biol.* 204, 3655-3682.
- Bejan, A. and Marden, J. H. (2006). Constructing animal locomotion from a ne thermodynamics theory. *Am. Sci.* 94, 342-349.
- Bell, G. (2001). Neutral macroecology. *Science* 293: 2413-2418.

- Biewener, A. A. (2003). Animal locomotion. New York: Oxford University Press.
- Biggs, D. C. (1977). Respiration and ammonium excretion by open ocean gelatinous zooplankton. *Limnol. Oceanogr.* 22: 108-117.
- Bochdansky, A. B., Deibel, D. (1999). Measurement of in situ clearance rates of *Oikopleura vanhoffeni* (Appendicularia : Tunicata) from tail beat frequency, time spent feeding and individual body size. *Mar. Biol.* 133: 37-44.
- Bone, Q. and Trueman, E. R. (1983). Jet propulsion in salps (Tunicata: Thaliacea). *J. Zool. Lond.* 201, 481-506.
- Bone, Q., Anderson, P. A. V. and Pulsford, A. (1980). The communication between individuals in salp chains. I. Morphology of the system. *Proc. R. Soc. B.* 210, 549- 558.
- Bone Q., Braconnot J. C., Carre C., Ryan K. P. (1997). On the filter-feeding of *Doliolum* (Tunicata: Thaliacea). *J. Exp. Mar. Biol. Ecol.* 214: 179-193.
- Bone Q., Braconnot J. C., Ryan K. P. (1991). On the pharyngeal feeding filter of the salp *Pegea confoederata* (Tunicata, Thaliacea). *Acta Zool.* 72: 55-60.
- Bone, Q., Carre, C. and Chang, P. (2003). Tunicate feeding filters. *J. Mar. Biol. Assoc. UK* 83, 907-919.
- Bone, Q., Carre, C. and Ryan, K. P. (2000). The endostyle and the feeding filter in salps (Tunicata). *J. Mar. Biol. Assoc. UK* 80, 523-534.
- Buesseler, K. O., Bauer, J. E., Chen, R.F., Eglinton, T. I., Gustafsson, O., Landing, W., Mopper, K., Moran, S. B., Santschi, P. H., Vernon Clark, R. and Wells, M. L.. (1996). An intercomparison of cross-flow filtration techniques used for sampling marine colloids: Overview and organic carbon results. *Mar. Chem.* 55: 1-31.
- Caron, D. A., Madin, L. P. and Cole, J. J. (1989). Composition and degradation of salp fecal pellets: Implications for vertical flux in oceanic environments. *J. Mar. Res.* 47(4): 829-850.
- Caron, D. A., Dam, H. G., Kremer, P., Lessard, E. J., Madin, L. P., Malone, T.C., Napp, J. M., Peele, E. R., Roman, M. R. and Youngbluth, M. J. (1995). The contribution of microorganisms to particulate carbon and nitrogen in surface waters of the Sargasso Sea near Bermuda. *Deep Sea Res. Part I* 42(6): 943-972.
- Cermeño, P. and Figueiras, F. G. (2008). Species richness and cell-size distribution: size structure of phytoplankton communities. *Mar. Ecol. Prog. Ser.* 357: 79-85.

- Cetta, C. M., Madin, L. P. and Kremer, P. (1986). Respiration and excretion by oceanic salps. *Mar. Biol.* 91: 529- 537.
- Cheng, J.-Y. and Demont, M. E. (1996). Jet-propelled swimming in scallops: swimming mechanics and ontogenic scaling. *Can. J. Zool.* 74, 1734- 1748.
- Colin S. P., Costello J. H. (2002). Morphology, swimming performance and propulsive mode of six co-occurring hydromedusae. *J. Exp. Biol.* 205: 427-437.
- Colin, S. P., Costello, J. H. and Klos, E. (2003). *In situ* swimming and feeding behavior of eight co-occurring hydromedusae. *Mar. Ecol. Prog. Ser.* 253, 305-309.
- Dabiri, J. O. (2009). Optimal vortex formation as a unifying principle in biological propulsion. *Annu. Rev. Fluid Mech.* 41, 17- 33.
- Dabiri, J. O. and Gharib, M. (2005). The role of optimal vortex formation in biological fluid transport. *Proc. R. Soc. B.* 272 (1572), 1557-1560.
- Dabiri, J. O., Colin, S. P. and Costello, J. H. (2006). Fast-swimming hydromedusae exploit velar kinematics to form an optimal vortex wake. *J. Exp. Biol.* 209 (11), 2025-2033.
- Dabiri, J. O., Colin, S. P., Costello, J. H. and Gharib, M. (2005). Flow patterns generated by oblate medusan jellyfish: field measurements and laboratory analyses. *J. Exp. Biol.* 208, 1257-1265.
- Daniel, T. L. (1983). Mechanics and energetics of medusan jet propulsion. *Can. J. Zool.* 61, 1406-1420.
- Daniel, T. L. (1985). Cost of locomotion: unsteady medusan swimming. *J. Exp. Biol.* 119, 149-164.
- Deibel, D. and Paffenhofer, G. A. (1988). Cinematographic analysis of the feeding mechanism of the pelagic Tunicate *Doliolum nationalis*. *Bull. Mar. Sci.* 43, 404-412.
- Dennett, M. R., Caron, D. A., Mursov, S., Polikarpov, I. G., Gavrilova, N. A., Georgieva, L.V. and Kuzmenko, L.V. (1999). Abundance and biomass of nano- and microplankton assemblages during the 1995 Northeast Monsoon and Spring Intermonsoon in the Arabian Sea. *Deep Sea Res. I.* 46: 1691-1717.

- Dewar, W. K., Bingham, R. J., Iverson, R.L., Nowacek, D. P., St Laurent, L.C. and Wiebe, P. H. (2006). Does the marine biosphere mix the ocean? J. of Mar. Res. 64: 541-561.
- Dusenbery, D. B. (2009). Living at the micro scale: The unexpected physics of being small. Cambridge: Harvard University press.
- Fedele, M. (1933). Sulla nutrizione degli animali pelagici III. Recherche sui Salpidae. Boll. Soc. di Nat. Napoli 45, 49-118.
- Fish, F. E. (1998). Comparative kinematics and hydrodynamics of odontocete cetaceans: morphological and ecological correlates with swimming performance. J. Exp. Biol. 201, 2867- 2877.
- Flood, P. R., Deibel, D. and Morris, C. C. (1990). Visualization of the transparent, gelatinous house of the pelagic tunicate *Oikopleura vanhoeffeni*. Biol. Bull. 178, 118-125.
- Fol, H. (1876). Ueber die Schleimdruse oder den Endostyl der Tunicaten. Morph. Jb. 1, 222-242.
- Fortier, L., Lefevre, J. and Legendre, L. (1994). Export of biogenic carbon to fish and to the deep-ocean: the role of large planktonic microphages. J. Plank. Res. 16(7): 809-839.
- Franqueville, C. (1971). Macroplankton profond (invertebres) de la mediterranee nordo-occidentale. Tethys 3, 11-56.
- Fuhrman, J. 2000. Impact of viruses on bacterial processes. In: Kirchman DL (ed) Microbial ecology of the oceans. Wiley-Liss, Inc., New York, pp 327-350.
- Gerritsen, J., and Porter, K. G. (1982). The role of surface chemistry in filter feeding by zooplankton. Science 216: 1225-1227.
- Gharib, M., Rambod, E. and Shariff, K. (1998). A universal time scale for vortex ring formation. J. Fluid Mech. 360, 121-140.
- Godeaux, J. (1998). The relationships and systematics of the Thaliacea, with keys for identification. In: Bone, Q. (ed.), The Biology of Pelagic Tunicates, Oxford University Press, New York, pp. 273- 294.
- Govindarajan, A. F., Bucklin, A. and Madin, L. P. (in review). A molecular phylogeny of the Thaliacea.

- Haddock, S. H. D., Heine, J. N. (2005). Scientific blue-water diving. Calif. Sea Grant, La Jolla, California.
- Hamner, W. M. (1975). Underwater observations of blue-water plankton: Logistics, techniques, and safety procedures for divers at sea. *Limnol. Oceanogr.* 20: 1045-1051.
- Hamner, W. M., Madin, L. P., Gilmer, R. W. and Hamner, P. P. (1975). Underwater observations of gelatinous zooplankton: sampling problems, feeding biology and behavior. *Limnol. Oceanogr.* 20, 907-917.
- Harbison, G. R. (1998). The parasites and predators of Thaliacea. In: Bone Q (ed) *The biology of pelagic tunicates*. Oxford University Press, New York, pp. 187-214.
- Harbison, G. R. and Campenot, R. B. (1979). Effects of temperature on the swimming of salps (Tunicata, Thaliacea): Implications for vertical migration. *Limnol. Oceanogr.* 24, 1081-1091.
- Harbison G. R., Gilmer R. W. (1976). The feeding rates of the pelagic tunicate *Pegea confederata* and two other salps. *Limnol. Oceanogr.* 21: 517-528.
- Harbison, G. R. and McAlister, V. L. (1979). The filter-feeding rates and particle retention efficiencies of three species of *Cyclosalpa* (Tunicata, Thaliacea). *Limnol. Oceanogr.* 24, 875-892.
- Harbison, G. R., McAlister, V. L. and Gilmer, R. W. (1986). The response of the salp, *Pegea confoederata*, to high levels of particulate material: starvation in the midst of plenty. *Limnol. Oceanogr.* 31, 371-382.
- Hirose E., Kimura S., Itoh T., Nishikawa J. (1999). Tunic morphology and cellulosic components of pyrosomas, doliolids, and salps (Thaliacea, Urochordata). *Biol Bull.* 196: 113-120.
- Huntley, M. E. and Zhou, M. (2004). Influence of animals on turbulence in the sea. *Mar. Ecol. Prog. Ser.* 273: 65-79.
- Hutchinson, G. E. (1961). The paradox of the plankton. *Amer. Nat.* 95: 137-145.
- Jorgensen, C. B. (1983). Fluid mechanical aspects of suspension feeding. *Mar. Ecol. Prog. Ser.* 11, 89-103.
- Katija, K. and Dabiri, J.O. (2009). A viscosity-enhanced mechanism for biogenic ocean mixing. *Nature* 460: 624-627.

- Kithil, P. W. 2006. Are salps a silver bullet against global warming and ocean acidification? AGU Fall Meeting, San Francisco.
- Kremer, P., and Madin, L. P. 1992. Particle retention efficiency of salps. *J. Plank. Res.* 14: 1009-1015.
- Krueger, P. S. Moslemi, A. A., Nichols, J. T., Bartol, I. K. and Stewart, W. J. (2008). Vortex rings in bio-inspired and biological jet propulsion. *Adv. Sci. Tech.* 58, 237- 246.
- Leibold, M. A. and McPeck, M. A. (2006). Coexistence of the niche and neutral perspectives in community ecology. *Ecology* 87: 1399-1410.
- Li, W. K. W. (1998). Annual average abundance of heterotrophic bacteria and *Synechococcus* in surface ocean waters. *Limnol. Oceanogr.* 43(7): 1746-1753.
- Madin, L. P. (1974). Field observations on the feeding behavior of salps (Tunicata: Thaliacea). *Mar. Biol.* 25: 143-147.
- Madin, L. P. (1982). Production, composition and sedimentation of salp fecal pellets in oceanic waters. *Mar. Biol.* 67: 39-45.
- Madin, L. P. (1990). Aspects of jet propulsion in salps. *Can. J. Zool.* 68, 765-777.
- Madin, L.P. and Cetta, C. M. (1984). The use of gut fluorescence to estimate grazing by oceanic salps. *J. Plankton Res.* 6: 475-492.
- Madin, L. P. and Deibel, D. (1998). Feeding and energetics of Thaliacea. In *The biology of pelagic tunicates*, (ed. Q. Bone), pp. 81-103. New York: Oxford University Press.
- Madin L. P. and Kremer P. (1995). Determination of the filter-feeding rates of salps (Tunicata, Thaliacea). *ICES J Mar Sci* 52: 583-595.
- Madin, L. P. and Purcell, J. E. (1992). Feeding, metabolism, and growth of *Cyclosalpa bakeri* in the subarctic Pacific. *Limnol. Oceanogr.* 37(6), 1236-1251.
- Madin, L. P. and Swanberg, N. R. (1984). In situ methods for the study of planktonic organisms. In *Divers, Submersibles and Marine Science*, vol. 9 (ed. N. C. Flemming), pp. 4-16. Memorial University, Newfoundland.
- Madin, L. P., Cetta, C. M. and McAlister, V. L. (1981). Elemental and biochemical composition of salps (Tunicata: Thaliacea). *Mar. Biol.* 63(3), 1432- 1793.

- Madin L. P., Kremer P., Hacker S. (1996). Distribution and vertical migration of salps (Tunicata, Thaliacea) near Bermuda. *J. Plankton Res.* 18: 747-755.
- Madin, L. P., Kremer, P., Wiebe, P. H., Purcell, J. E., Horgan, E. H. and Nemanzie, D. A. (2006). Periodic swarms of the salp *Salpa aspera* in the Slope Water off the NE United States: Biovolume, vertical migration, grazing, and vertical flux. *Deep Sea Res. I.* 53, 804-819.
- McKenna, S. P. and McGillis, W. R. (2002). Performance of digital image velocimetry processing techniques. *Exp. Fluids* 32, 106-115.
- Metcalf, M. M. (1918). The Salpidae: A taxonomic study. *Bull. U.S. Natl. Museum* 100, 1-193.
- Montagnes, D. J. S., Berges, J. A., Harrison, P. J. and Taylor, F. J. R. (1994). Estimating carbon, nitrogen, protein, and chlorophyll *a* from volume in marine phytoplankton. *Limnol. Oceanogr.* 39(5): 1044-1060.
- Morris C. C., and Deibel, D. (1993). Flow rate and particle concentration within the house of the pelagic tunicate *Oikopleura vanhoeffeni*. *Mar. Biol.* 115: 445-452.
- Nauen, J. C. and Lauder, G. V. (2002). Quantification of the wake of rainbow trout (*Oncorhynchus mykiss*) using three-dimensional stereoscopic digital particle image velocimetry. *J. Exp. Biol.* 205, 3271-3279.
- Nishikawa, J. and Terazaki, M. (1995). Measurement of swimming speeds and pulse rate of salps using a video equipment. *Bull. Plankton Soc. Japan* 41: 170-173.
- Pace, M. L. and Bailiff, M. D. (1987). Evaluation of a fluorescent microsphere technique for measuring grazing rates of phagotrophic microorganisms. *Mar. Ecol. Prog. Ser.* 40, 185-193.
- Partensky, F., Hess, W. R., and Vaulot, D. (1999). *Prochlorococcus*, a marine photosynthetic prokaryote of global significance. *Microbiol. Molec. Biol. Rev.* 63(1): 106-127.
- Phillips, B., Kremer, P. and Madin, L. P. (2009). Defecation by *Salpa thompsoni* and its contribution to vertical flux in the Southern Ocean. *Mar. Biol.* 156: 455-467.
- Prasad, A. K. (2000). Particle image velocimetry. *Curr.Sci.* 79, 51-60.
- Rubenstein, D. I. and Koehl, M. A. R. (1977). The mechanisms of filter feeding: some theoretical considerations. *Am. Nat.* 111, 981-994.

- Shimeta, J. and Jumars, P. A. (1991). Physical mechanisms and rates of particle capture by suspension feeders. *Oceanogr. Mar. Biol.* 29, 191-257.
- Siekman, J. (1963). On a pulsating jet from the end of a tube, with application to the propulsion of certain aquatic animals. *J. Fluid Mech.* 15, 399-418.
- Silver, M. W. and Bruland, K. W. (1981). Differential feeding and fecal pellet composition of salps and pteropods, and the possible origin of deep-water flora and olive-green "cells". *Mar. Biol.* 62, 263-273.
- Silvester, N. R. (1983). Some hydrodynamic aspects of filter feeding with rectangular-mesh nets. *J. theor. Biol.* 103, 265-286.
- Stamhuis, E. J. and Videler, J. J. (1995). Quantitative flow analysis around aquatic animals using laser sheet Particle Image Velocimetry. *J. Exp. Biol.* 198, 283-294.
- van Duren L. A., Stamhuis, E. J., Videler, J. J. (2003). Copepod feeding currents: flow patterns, filtration rates and energetics. *J. Exp. Biol.* 206: 255-267.
- Vargas, C. A. and Madin, L. P. (2004). Zooplankton feeding ecology: clearance and ingestion rates of the salps *Thalia democratica*, *Cyclosalpa affinis* and *Salpa cylindrica* on naturally occurring particles in the Mid-Atlantic Bight. *J. Plankton Res.* 26, 827-833.
- Visser, A. W. (2007). Biomixing of the oceans? *Science* 316: 838-839.
- Visser, A. W., and T. Kiorboe. (2006). Plankton motility patterns and encounter rates. *Oecologia* 148(3): 538-546.
- Vogel, S. (1994). *Life in moving fluids : the physical biology of flow*. Princeton, N.J.: Princeton University Press.
- Vogel, S. (2003). *Comparative biomechanics*. Princeton, N.J.: Princeton University Press.
- Weihs, D. (1977). Periodic jet propulsion of aquatic creatures. *Fortschr. Zool.* 24, 171-175.
- Whitehouse, B. G., Yeats, P. A., and Strain, P. M. (1990). Cross flow filtration of colloids from aquatic environments. *Limnol. Oceanogr.* 35: 1368-1375.
- Wiebe, P. H., Madin, L. P., Haury, L. R., Harbison, G. R. and Philbin, L. M. (1979). Diel vertical migration by *Salpa aspera* and its potential for large-scale particulate organic matter transport to the deep sea. *Mar. Biol.* 53, 249-255.

- Yamasaki, A., Fukuda, H., Miyajima, T., Nagata, T., Ogawa, H. and Koike, I. (1998). Submicrometer particles in northwest Pacific coastal environments: Abundance, size distribution, and biological origins. *Limnol. Oceanogr.* 43(3): 536-542.
- Yen, J., Brown, J., Webster, D. R. (2003). Analysis of the flow field of the krill, *Euphausia pacifica*. *Mar. Fresh. Behav. Physiol.* 36: 307-319.
- Yoon, W. D., Marty, J. C., Sylvain, D. and Nival, P. (1996). Degradation of faecal pellets in *Pegea confoederata* (Salpidae, Thaliacea) and its implication in the vertical flux of organic matter. *J. Exp. Mar. Biol. Ecol.* 203(2): 147-177.
- Yount, J. L. (1954). The taxonomy of the Salpidae (Tunicata) of the Central Pacific Ocean. *Pac. Sci.* 3: 276- 330.
- Yount, J. L. (1958). Distributions and ecologic aspects of central Pacific Salpidae (Tunicata). *Pac. Sci.* 12, 111-130.

REPORT DOCUMENTATION PAGE	1. REPORT NO. MIT/WHOI 2010-01	2.	3. Recipient's Accession No.
4. Title and Subtitle Form, function and flow in the plankton: Jet propulsion and filtration by pelagic tunicates			5. Report Date February 2010
			6.
7. Author(s) Kelly Rakow Sutherland			8. Performing Organization Rept. No.
9. Performing Organization Name and Address MIT/WHOI Joint Program in Oceanography/Applied Ocean Science & Engineering			10. Project/Task/Work Unit No. MIT/WHOI 2010-01
			11. Contract(C) or Grant(G) No. (C) OPP-0338290 OCE-0647723 (G)
12. Sponsoring Organization Name and Address National Science Foundation WHOI Academic Programs Office MIT			13. Type of Report & Period Covered Ph.D. Thesis
			14.
15. Supplementary Notes This thesis should be cited as: Kelly Rakow Sutherland, 2009. Form, function and flow in the plankton: Jet propulsion and filtration by pelagic tunicates. Ph.D. Thesis. MIT/WHOI, 2010-01.			
16. Abstract (Limit: 200 words) Trade-offs between filtration rate and swimming performance among salp species with distinct morphologies and swimming styles were compared. Time-varying body volume calculated from <i>in situ</i> video sequences resulted in higher filtration rates than previous measurements, setting an upper limit on filtration capacity. Though each species possessed a unique combination of body kinematics, normalized filtration rates were comparable across most species suggesting a common flow optimum. <i>In situ</i> dye visualization and Particle Image Velocimetry measurements were used to describe jet wake properties and swimming performance variables. All species swam via vortex ring propulsion. Though <i>Weelia cylindrica</i> was the fastest swimmer, <i>Pegea confoederata</i> was the most efficient, producing the highest weight-specific thrust and whole-cycle propulsive efficiency. Weak swimming performance parameters in <i>Cyclosalpa affinis</i> , including low weight-specific thrust and low propulsive efficiency, may be compensated by low energetic requirements. A low Reynolds number mathematical model using realistic oceanic particle-size concentrations, and feeding experiments with 0.5, 1 and 3 µm microspheres, showed that submicron particles are encountered at higher rates than larger particles. Though 1- 10 µm-sized particles provide four times as much carbon as 0.1- 1 µm- sized particles, particles smaller than the mesh size (1.4 µm) can still satisfy salp energetic needs.			
17. Document Analysis <div style="display: flex; justify-content: space-between;"> <div> a. Descriptors propulsion salp filtration b. Identifiers/Open-Ended Terms c. COSATI Field/Group </div> </div>			
18. Availability Statement Approved for publication; distribution unlimited.		19. Security Class (This Report) UNCLASSIFIED	21. No. of Pages 99
		20. Security Class (This Page)	22. Price